END
DATE
FILMED
11 87

AD-A185 250

CONTRACT NO. DAJA45-84-C-0045

OPTICALLY TUNED MM-WAVE IMPATT SOURCE

FINAL REPORT   JULY 1987

87   9 14 028

CONTRACT NO. DAJA45-84-C-0045

OPTICALLY TUNED MM-WAVE IMPATT SOURCE

FINAL REPORT   JULY 1987

Marconi Electronic Devices Ltd.,
Doddington Road,
Lincoln LN6 3LF
England.

Dept. of Electronic & Electrical Eng.,
University College London,
Torrington Place,
London WC1E 7JE,
England.

DTIC
ELECTE
S SEP 2 3 1987 **D**
D CR

Prepared by:

Miss S.P. Brunt   MEDL
Miss J. Taylor   "
Mr. I. Dale   "
Dr. J.F. Singleton   "

Dr. A.J. Seeds   UCL

REPORT DOCUMENTATION PAGE

1a REPORT SECURITY CLASSIFICATION UNCLASSIFIED		1b. RESTRICTIVE MARKINGS			
2a SECURITY CLASSIFICATION AUTHORITY		3. DISTRIBUTION / AVAILABILITY OF REPORT Approved for public release; distribution unlimited			
2b. DECLASSIFICATION / DOWNGRADING SCHEDULE					
4 PERFORMING ORGANIZATION REPORT NUMBER(S)		5. MONITORING ORGANIZATION REPORT NUMBER(S) R&D 4426-EE-01			
6a. NAME OF PERFORMING ORGANIZATION Marconi Electronic Devices	6b. OFFICE SYMBOL (If applicable)	7a. NAME OF MONITORING ORGANIZATION USARDSG-UK			
6c. ADDRESS (City, State, and ZIP Code) Doddington Road Lincoln, LN6 0LF		7b. ADDRESS (City, State, and ZIP Code) Box 65 FPO NY 09510-1500			
8a. NAME OF FUNDING / SPONSORING ORGANIZATION USARDSG-UK ARO-E	8b. OFFICE SYMBOL (If applicable)	9. PROCUREMENT INSTRUMENT IDENTIFICATION NUMBER DAJA45-84-C-0045			
8c. ADDRESS (City, State, and ZIP Code) Box 65 FPO NY 09510-1500		10. SOURCE OF FUNDING NUMBERS			

PROGRAM ELEMENT NO.	PROJECT NO.	TASK NO	WORK UNIT ACCESSION NO
398548	1L161102BH5	0	

11. TITLE (Include Security Classification)
(U) Optically Tuned MM-Wave IMPATT Source

12 PERSONAL AUTHOR(S)
Mr. D.A. Williams

13a. TYPE OF REPORT Final	13b. TIME COVERED FROM _____ TO _____	14. DATE OF REPORT (Year, Month, Day) July 1987	15 PAGE COUNT 411

16 SUPPLEMENTARY NOTATION

17	COSATI CODES		18. SUBJECT TERMS (Continue on reverse if necessary and identify by block number)
FIELD	GROUP	SUB-GROUP	
09	01		

19 ABSTRACT (Continue on reverse if necessary and identify by block number)

The analytic theory of optical tuning in IMPATT oscillators developed in the initial phase of the work has been extended and generalised. Accuracy of the theory in predicting tuning at the higher oscillator voltage swings has been greatly improved by reformulating the Bessel function series used to express avalanche gain. A model for optical injection locking, where the oscillator output is locked to a microwave intensity modulated optical signal, has also been developed. The computer model for optical control has been modified to study the tuning behaviour of Ku-Band IMPATTs, as used in the recent experimental work. Work on optical tuning speed studies has also been extended. The experimental progam has produced a number of developments. A delay line discriminator has been used to measure the tuning speed in response to a step change in illumination level. It has been found that a frequency shift of 1.4MHz at W-Band could be achieved in less than 20ns and a frequency shift of 5.6MHz at Ka-Band in less than 10ns. However both of these results are thought to be due to limitations in the measurement system rather than in the intrinsic response time. Nonetheless, these results

20 DISTRIBUTION / AVAILABILITY OF ABSTRACT ☒ UNCLASSIFIED/UNLIMITED ☐ SAME AS RPT ☐ DTIC USERS	21 ABSTRACT SECURITY CLASSIFICATION Unclassified	
22a NAME OF RESPONSIBLE INDIVIDUAL Dr John M. Zavada	22b TELEPHONE (Include Area Code) 01-409 4423	22c OFFICE SYMBOL AMXSN-UK-RI

DD FORM 1473, 84 MAR

83 APR edition may be used until exhausted
All other editions are obsolete

Block 19 Cont/...

are valuable in that they confirm that the tuning response is not associated with trapping
or other slow effects. A special Ka-Band IMPATT structure was fabricated using a modified
integral heat sink process to produce a 40 pm diameter hole beneath the P^+ region of the
diode through which the diode could be illuminated. Comparative tests showed that the
tuning slope was improved with through heat-sink illumination by almost an order of
magnitude. Finally, modifications to edge illumination techniques for IMPATT diodes have
been investigated including the use of quartz stand-off rather than quartz ring mounting.
Also, a technique for reducing the diameter of optical fibres by wet chemical etching has
been developed, which has applications in a number of illumination configurations.

DISTRIBUTION

Fiscal Officer (24 copies)   U.S. Army Research, Development
                               and Standardisation Group,
                               London

Dr. A.J. Seeds   University College London

Dr. J.F. Singleton   MEDL Lincoln
S. Brunt   "   "
D.A. Williams   "   "
I. Dale   "   "
J. Taylor   "   "
S. Neylon   "   "
E. Smith   "   "
Dr. J. Ondria   "   "

1.   Contract Objectives

The objective of the contract was to extend the work of the earlier feasibility
study[1] on the control of the operating frequency of millimetre-wave IMPATT
oscillators using an optical signal. Specific objectives were to maximise the
frequency tuning obtainable with conventional IMPATT structures, to fabricate a
special IMPATT structure designed for optical control and to examine tuning
speed and noise performance.

2.   Summary of Principal Results

The analytic theory of optical tuning in IMPATT oscillators developed in the
initial phase of the work [1] has been extended and generalised. Accuracy of
the theory in predicting tuning at the higher oscillator voltage swings has been
greatly improved by reformulating the Bessel function series used to express
avalanche gain. A model for optical injection locking, where the oscillator
output is locked to a microwave intensity modulated optical signal, has also been
developed.

The computer model for optical control has been modified to study the tuning
behaviour of Ku-Band IMPATTs, as used in the recent experimental work. Work
on optical tuning speed studies has also been extended.

The experimental programme has produced a number of developments. A delay
line discriminator has been used to measure the tuning speed in response to a
step change in illumination level. It has been found that a frequency shift of
1.4MHz at W-Band could be achieved in less than 20ns and a frequency shift of
5.6MHz at Ka-Band in less than 10ns. However both of these results are thought
to be due to limitations in the measurement system rather than in the intrinsic
response time. Nonetheless these results are valuable in that they confirm that
the tuning response is not associated with trapping or other slow effects.

A special Ka-Band IMPATT structure was fabricated, using a modified integral
heat sink process to produce a 40 μm diameter hole beneath the P^+ region of the

1.

diode through which the diode could be illuminated. Comparative tests showed that the tuning slope was improved with through heat-sink illumination by almost an order of magnitude.

Finally modifications to edge illumination techniques for IMPATT diodes have been investigated including the use of quartz stand-off rather than quartz ring mounting. Also a technique for reducing the diameter of optical fibres by wet chemical etching has been developed, which has applications in a number of illumination configurations.

3.   Analytic Theory

When the electric field in an IMPATT diode is above the breakdown value charge carriers, whether optically generated or not, experience avalanche multiplication. This avalanche multiplication was represented in the earlier theory [1] by truncated Bessel function series of argument.

$$X = \frac{2(m+1)V_1}{\omega\tau_a V_b} \qquad \text{.......(1)}$$

where m is an ionisation non-linearity constant ($m \approx 6$ for silicon), V_1 is the peak value of the modulated component of the voltage across the IMPATT, V_b is the breakdown voltage, ω the operating frequency and τ_a the avalanche zone transit time, and where it is assumed that the device remains punched through over the whole cycle.

As the voltage swing across the device increases higher order Bessel function coefficients become significant and the truncated series give a poorer representation of the effect of avalanche multiplication. The extended analytic theory uses more general expressions which are capable of good accuracy over a wide range of voltage swings.

At the same time the opportunity was taken to extend the theory to treat optical injection locking.

2.

In optical injection locking the optical control signal is intensity modulated at a frequency close to the free-running frequency of the IMPATT oscillator[2]. Although the technique has yet to be demonstrated at millimetre-wave frequencies due to the difficulty of intensity modulating the control signal at such high rates, developments in optical heterodyne technology[3] suggest that the technique could offer novel systems possibilities in the future.

The derivation of the extended theory is given in Appendix A; only the most important results will be discussed here. Considering first optical tuning: the change in oscillation frequency for a small change in optically generated current, is given by:

$$\delta\omega = \frac{F_a\{X\}}{Q\, I_{dc}\, \tau_a} \delta\, I_{so} \qquad \ldots\ldots(2)$$

where Q is the oscillator Q, I_{dc} the oscillator bias current and $F_a\{X\}$ is an avalanche gain term. Comparison with equation 4.26 of [1] shows that the only difference lies in the definition of the avalanche gain parameter $F_a\{X\}$.

Figure 1a shows the dependence of $F_a\{X\}$ on X as an increasing number of terms in the Bessel function series defining $F_a\{X\}$ (see equation 10 of Appendix A) are taken into account. To appreciate the practical significance of these curves X must be related to the oscillator voltage swing through equation (1). For a typical uniformly doped device $\tau_a \simeq 0.2\ \pi/\omega$ which with m = 6 gives

$$X \simeq 22\, \frac{V_1}{V_b} \qquad \ldots\ldots(3)$$

The earlier theory corresponds to the curve n ⩽ 1: this becomes seriously in error for X > 3.0, corresponding to > 14% voltage modulation. Curves for n ⩽ 2 or 3 give satisfactory accuracy for up to 25% voltage modulation, the highest

3.

value likely to be used in uniformly doped structures.

For optical injection locking the full locking range is given by

$$2\Delta\omega_L \;=\; 5\ F_b\ \{x\}\ \frac{I_o\ \{x\}\omega_o}{I_1\ \{x\}\ Q\ I_{dc}}\ \ I_{S1} \qquad \ldots\ldots(4)$$

where $I_n\ \{x\}$ are modified Bessel functions and $F_b\ \{X\}$ is an avalanche gain parameter. The optical injection locking range is proportional to the peak optically injected locking current I_{S1}. Figure 1b shows the dependence of $F_b\ \{X\}$ on X. From equation (3) $F_b\ \{X\} = 250$ for 20% voltage modulation; this avalanche gain renders IMPATT diodes particularly suitable for optical control.

As a numerical example, consider a Ka-Band oscillator having $\omega_o = 2^\pi$ x 3.8 x 10^{10} r s^{-1}, Q = 100 and I_{dc} = 100mA.

With 20% voltage modulation and a peak optically injected locking current of 100 µA the predicted full locking range would be 540MHz, a practically useful value.

4.   Computer Modelling Studies

Because of the decision to broaden the work to include Ka-Band IMPATTs the parameters of the model had to be changed. However the basic model described in section 5.1 of [1] was retained.

4.1.   Device parameters

The Ka-Band devices used in the experimental work were silicon, uniformly doped P^+NN^+ structures. The material parameters of [1] were retained, with an assumed junction temperature of 450K. A complementary error function model for the doping profile gave a

satisfactory match to the measured values using the parameters listed below in equation (5.7) of [1]:

$$N_e = 3.00 \times 10^{16} \text{ cm}^{-3}$$

$$N_d = 4.00 \times 10^{19} \text{ cm}^{-3}$$

$$N_a = 1.00 \times 10^{20} \text{ cm}^{-3}$$

$$W = 1.40 \times 10^{-4} \text{ cm}$$

$$W_d = 3.10 \times 10^{-6} \text{ cm}$$

$$W_a = 1.00 \times 10^{-5} \text{ cm}$$

Figure 2 shows the modelled profile and Figure 3 the measured profile; agreement is seen to be satisfactory.

4.2.   DCP Results

A bias current density of 4,000 A cm^{-2} was selected for the modelling work, corresponding to a bias current of 112mA in the experimental devices.

Figure 4 shows the electric field and electron current density profiles for the device. The diode is seen to be punched-through, thus minimising losses in undepleted material. Applying the 20%-80% criterion to the electron current density curve suggests an avalanche zone length, $L_a = 0.23\mu\text{m}$.

The predicted bias voltage was 29.5V with the diode not oscillating, a value in satisfactory agreement with measured values for the experimental oscillators of around 25V when allowance is made for back-bias effects.

4.3. SSP results

The small signal admittance of the IMPATT diode was evaluted over the frequency range 30 to 50GHz.

Figure 5a shows an admittance plot for the unilluminated diode. The conductance is seen to be negative over the full frequency range. Figure 5b shows an admittance plot for an optically generated hole current (corresponding to illumination from the N^+ direction) of 50A cm^{-2} (equivalent to a current of 1.43mA in a device of the area used experimentally). The magnitude of the diode conductance is seen to be reduced and the susceptance changed. Figure 5c shows an admittance plot for an optically generated electron current of 50A cm^{-2} (corresponding to illumination from the P^+ direction). The change in admittance is seen to be much greater than for hole injection, confirming the effect of the higher avalanche ionisation coefficient for electrons in silicon.

4.4. FSP Results

Reference to equation 2 shows that the oscillator frequency change for a given optically generated current is expected to be inversely proportional to oscillator Q. An object of the large signal modelling work was to investigate the effect of changing the oscillator Q on optical control performance. For this purpose two different oscillator circuits were used. The first circuit, shown in Figure 6a, is similar to that used in the previous W-Band work (see Figure 5.7 of [1]). It consists of an inductor, L_p, selected to cancel the capacitive susceptance of the diode at the oscillation frequency with a quarter-wave transformer to match the diode admittance to that of the load.

Close to resonance the quarter-wave transformer and load can be represented as a series L-C-R circuit, following the derivation of

6.

Appendix 5, where

$$L_e = \frac{Z_t}{8f_o} \qquad \ldots\ldots(5)$$

$$C_e = \frac{2}{\pi^2 f_o Z_t} \qquad \ldots\ldots(6)$$

$$R_e = \frac{Z_t^2}{Z_L} \qquad \ldots\ldots(7)$$

with f_o being the resonant frequency, Z_t the characteristic impedance of the transformer and Z_L the load impedance.

Thus the oscillator Q can be written

$$Q = \frac{\omega (L_p + L_e)}{R_e + R_p} \qquad \ldots\ldots(8)$$

where ω is the oscillation frequency. For $\omega = 2\pi f_o$ L_e is series resonant with C_e and an equivalent admittance is presented to the diode by the circuit of Figure 6b. The Q for this circuit is given by

$$Q = \frac{\omega L_p}{R_e + R_p} \qquad \ldots\ldots(9)$$

and is therefore less than that for the circuit of Figure 6a, although the admittance presented to the diode is the same, giving equivalent oscillation conditions.

7.

For oscillation at Ka-Band the following values were chosen:

$$R_p = 1.0$$

$$L_p = 0.085 \text{ nH}$$

$$C = 15\text{pF}$$

$$Z_L = 50$$

$$Z_t = 15$$

giving $R_e = 4.5$ and $L_e = 0.049\text{nH}$ at the design frequency, $f_o = 38\text{GHz}$. Thus the Q for the circuit of Figure 6a, from equation 8, is 5.82 while for that of Figure 6b, from equation 9, it is 3.69.

A device area of $2.8 \times 10^{-5} \text{ cm}^2$ was used throughout the modelling work, corresponding to the mesa diameter of about $60\mu\text{m}$ used experimentally. For the high Q circuit with no optically generated current the oscillation stabilised at a frequency of 38.708GHz with 15.6% voltage modulation, while for the low Q circuit the frequency of oscillation was 39.197GHz with 16.2% voltage modulation. The values are not identical because the quarter-wave transformer is being operated slightly off its resonant frequency of 38GHz.

Figure 7 shows the change in oscillation frequency for the two circuits with an optically injected current comprising equal numbers of electrons and holes. The tuning slope for the low Q circuit is 11.9MHz mA^{-1} while that for the high Q circuit is 7.9MHz mA^{-1}, a ratio of 1.51. The ratio of the circuit Q factors is 1.58 thus confirming very satisfactorily the prediction of equation 2.

Attempts were made to model high Q circuits representing those used in the experimental work. However, it was found that the circuit

8.

configurations available in the model gave rise to sub-harmonic instabilities when the necessary additional elements were introduced and modifications to the program would be necessary to give a more general oscillator circuit model. Since these modifications would increase program execution time considerably they have not been implemented as part of this study.

The FSP was also used to carry out a more detailed investigation of optical tuning transients. Figure 8 shows the tuning transient resulting from a step function optical input producing 5A cm^{-2} in the low Q oscillator circuit. As expected electron injection produces a larger tuning effect than hole injection, owing to the larger avalanche ionisation coefficient for electrons than for holes in silicon. The exact shape of the initial transient depends on the point in the oscillation cycle when the optical signal is applied. Clearly, tuning is very fast; 90% of the frequency change takes place in less than 0.5ns.

Figure 9 shows optical tuning transients for step function inputs to the high Q oscillator circuit. Again electron injection produces a much larger tuning effect. The curves for hole injection currents of 5 and 10A cm^{-2} verify that the change in frequency is proportional to the injected current. The time taken for 90% of the frequency change to take place is about 0.2ns, and this seems independent of the magnitude of the change.

The reason for the difference in tuning speed between the two circuits is not clear, since the stored energy in the low Q circuit would be expected to be smaller. It is possible that the time at which the control signal has been applied is less favourable in the first case. Further examination of the effect of applying the tuning signal at different points in the oscillation cycle is needed to clarify the situation. What can be asserted with confidence is that the tuning is fast relative to conventional oscillator control techniques.

9.

5.   Experimental Work

5.1.   Device Fabrication

A shift of emphasis to Ka-Band took place as part of the present
programme. This involved the fabrication of new IMPATT structures
including a special device design allowing illumination from beneath the
heatsink.

Figure 10 shows the basic mesa structure. The epitaxial layer was
grown by VPE on an N^+ substrate of doping density 4.0×10^{19} cm^{-3}. An
N layer doping density of 3.0×10^{16} cm^{-3} was used. The P^+ layer was
produced by boron diffusion with a surface concentration of 1.0×10^{20}
cm^{-3}. A Cr-Au contact was evaporated onto the P^+ surface and the
heatsink plated over this layer before mesa etching and cleaving. Mesa
diameters used ranged from 50 to 65 μm giving device areas of from
1.96×10^{-5} to 3.3×10^{-5} cm^2.

In order to permit illumination from the P^+ region special IMPATT
structures were fabricated using a modified integral heat sink process to
produce a 25μm diameter hole beneath the device. Figure 11 is a
drawing of the modified device while Figures 12 to 15 are scanning
electron micrographs of a typical experimental device. The doping
profiles for these devices were similar to the conventional structures,
with a typical junction area of 2.85×10^{-5} cm^2.

5.2.   Optical Tuning Results

The difficulties caused by refraction in the quartz ring package were
referred to in [1]. For the present work 250μm quartz stand-off blocks
were used to permit direct optical access to the active device.

As in the earlier W-Band work resonant cap oscillator circuits were used
[8]. For the conventional devices a 50/125 μm fibre was aligned

perpendicular to the plane of the junction using an XYZ stage. With this configuration optically generated currents of up to $31\,\mu A$ were achieved using a semiconductor laser source of emission wavelength 850nm and output power 2.9 mW. Assuming an internal quantum efficiency of unity, which is a reasonable approximation at this wavelength, the coupling efficiency is given by

$$\eta_c = \frac{I_{so}hc}{e\,\lambda\,P_{op}} \qquad\qquad ......(10)$$

where I_{so} is the optically generated current, P_{op} the optical power, λ the optical wavelength, h Planck's constant, e the electronic charge and c the velocity of light in vacuo. For the values quoted above η_c is 1.6%. This value is about 50% better than that obtained using the quartz ring package and W-Band diodes [1] but is still very low.

Light emerging from the cleaved end of the fibre diverges with an angle of about 35°. The structure of the diode mount requires the end of the fibre go be at least 125μm from the diode mesa, giving a beam area at the mesa edge of $12,300\,\mu m^2$. Since the diode is about $60\,\mu m$ in diameter and $5\,\mu m$ high, the coupling efficiency cannot exceed 2.4%. Account also needs to be taken of the reflection loss at the air/silicon interface. For normal incidence this is given by the Fresnel equation

$$\eta_r = 1 - \left(\frac{n_s - 1}{n_s + 1}\right)^2 \qquad\qquad ......(11)$$

where n_s is the refractive index of silicon.
Using $n_s = 3.44$ gives $\eta_r = 70\%$. Thus the overall coupling efficiency would be 1.7%, a value in reasonable agreement with the measured results. Any slight tilting of the diode mount will shade part of the diode lowering the coupling efficiency further. Note that this calculation ignores recombination in the substrate of the diode: since the diffusion length in heavily doped N type silicon is of the order of

11.

$20\,\mu$m this is a good approximation. It is also assumed that all of the light incident on the diode is absorbed; this is justified since the absorption length in silicon for a wavelength of 850nm is about $10\,\mu$m, a value small relative to the mesa diameter.

Figure 16 shows an optical tuning curve for a Ka-Band oscillator under edge illumination. The maximum frequency tuning obtained was 40MHz, some four times greater than in the earlier W-Band work [1]; a tenfold increase in percentage tuning.

The oscillator Q was measured by injection locking to be about 30, which with an estimated voltage modulation of 15% and the avalanche zone length estimated in section 4.2 gives a predicted tuning slope of 1.2MHz μA^{-1}; this is in reasonable agreement with the measured value of 1.5MHz μA^{-1}.

Some preliminary measurements on the modified IMPATT structure were made. Light was incident on the underside of the diode through the mount shown in Figure 17. Alignment of the core of the fibre was very difficult to achieve and the maximum optically generated current obtained was $1.4\,\mu$A. This low value results from the fibre end being some 100μm from the device. Allowing for the beam divergence from the end of the fibre would give a beam area at the device of about $9,000\,\mu$m^2: because of the limited diameter of the hole in the diode mount considerable scattering from the walls of the hole takes place. The hole diameter in the IMPATT integral heatsink is $25\,\mu$m, giving an area available for illumination of $490\,\mu$m^2. Thus the coupling efficiency cannot exceed 5%. From equation 10 the measured coupling efficiency was about 0.1%. Allowing for reflection loss at the air/silicon interface only reduces the discrepancy slightly. It is thought that a considerable improvement in coupling efficiency could be obtained using a micro-positioning system for fibre alignment.

Although the optically generated current was small, significant tuning

12.

was observed. Figure 18 shows a measured tuning characteristic. The measured tuning slope was $3.1\text{MHz}\,\mu A^{-1}$. This is about double the tuning slope for edge illumination of similar devices. When account is taken of the lower bias current, and hence reduced output power and avalanche gain coefficient, $F_a\{X\}$, the increased tuning slope is more significant still. The explanation for this is probably the increase in the proportion of optically generated electron current entering the avalanche zone, resulting from illumination from the P^+ direction. This could be investigated by using shorter wavelength light to concentrate absorption in the P^+ region.

5.3.   Tuning Speed Measurements

Measurements of optical tuning speed were carried out for both W-Band and Ka-Band oscillators. The laser was biased above threshold and driven with pulses of $1\mu s$ duration and 5ns rise time. The change in IMPATT oscillator frequency was measured using the delay line discriminator system shown in Figure 19.

Figure 20 shows the optical tuning transient for a W-Band oscillator. The frequency change of 1.4MHz took place in under 20ns. Figure 21 shows the tuning transient for a Ka band oscillator. The frequency change of 5.5MHz took place in about 8ns.

In both of these results the rise time of the bias pulse was a significant limiting factor. When biased above threshold the laser output rise time would be expected to be under 1ns. The combined discriminator delay and oscilloscope rise time was about 4.5ns for the W-Band system and 6ns for the Ka-Band system. Thus the Ka-Band result is at the measuring limit of the test set-up, while the W-Band result, which was for a high Q oscillator circuit $(Q \simeq 200)$, is somewhat slower. Both results are valuable in that they confirm that slow processes, such as trapping, are not significant in the optical tuning results presented.

13.

5.4.   Etching of Optical Fibre

As discussed in Section 5.2 there were considerable difficulties in locating the optical fibre close to the underside of the IMPATT structure so as to achieve base illumination. Since the cladding of the fibre was of diameter 125 μm, with a core diameter of 50 μm, considerable scope exists for reducing the cladding diameter without impairing the optical confinement. The fibre could then be located immediately under the device integral heat sink.

The method used to reduce the fibre diameter was wet chemical etching with a 1:9 mixture of hydrochloric and hydrofluoric acid. An etch rate of 25 μm diameter/15minutes was observed, with excellent uniformity. Figure 22 shows the transition between the etched and unetched fibre. This technique will be useful in further work on base illumination.

6.   Conclusions

A detailed analytic theory for the optical control of IMPATT diodes has been developed. This shows that avalanche multiplication of the optically generated carriers constitutes an important gain mechanism, making IMPATT devices especially suitable for optical control. For a typical Ka-Band oscillator of Q factor 30 a 1% change in frequency is predicted for an optically generated current of less than 400 μA: this could be produced by a 1mW laser given good coupling efficiency.

Calculations of optical injection locking range predict that for a similar oscillator a range of 5% should be achievable with a peak injected locking current of 100 μA.

The analytic theory suffers two main limitations. First, the power law avalanche ionisation coefficient model does not account for saturation at high electric fields; this makes the predictions somewhat optimistic at high voltage swings. Second, the theory assumes equal avalanche ionisation coefficients for holes and

14.

electrons. This is cannot account for variations in the composition of the optically generated current entering the avalanche zone, resulting from different illumination configurations.

To remove these limitations and to permit studies of transient effects a comprehensive computer model has been devloped. Among the important results obtained is that the optical tuning slope for electron injection to the avalanche zone of a silicon IMPATT is about four times that for hole injection; a consequence of the different ionisation coefficients for electrons and holes in silicon. Studies of the small signal admittance over a wide frequency range have confirmed the greater effect of electron injection. A comparative study of two oscillator circuits of different Q factor has been made. This confirmed the Q^{-1} dependence of the tuning slope predicted by the analytic theory.

Further transient tuning studies have been carried out. These confirm that sub-nano-second tuning speeds are readily possible. However, the reasons for the different tuning speed behaviour of the two oscillator circuits examined is not well understood. Further tests, coupled with an extended measurement programme would be needed to clarify this issue.

A major advance in the experimental work has been the fabrication of a special IMPATT structure permitting illumination of the P^+ region of the device. Preliminary results indicate an improved tuning slope relative to edge illumination. However, the tuning range was severely limited owing to difficulties in bringing the fibre end close enough to the device to give efficient coupling. A wet etching technique has been developed for reducing the diameter of the fibre end, and this, combined with refinements to the alignment procedure, would be expected to give much improved coupling efficiency. An important area for further work is the assessment of the thermal performance of the special IMPATT structure.

Removal of part of the integral heat-sink would be expected to lead to a deterioration in output power capability. It was possible to obtain current densities sufficient for oscillation in the experimental devices. However, a

15.

detailed assessment of power output, temperature and reliability would be very useful.

Work on edge illumination has continued, including the development of a quartz stand-off package which permits direct illumination of the device. This has enabled a tuning range of 40MHz to be obtained at Ka-Band, an improvement of an order of magnitude in percentage tuning over earlier W-Band results using a quartz ring package. There remains much scope for further improvement in coupling efficiency, which could enhance the tuning ranges obtained by a factor of over 50. Suggested techniques would include the use of fibre microlenses to give shaped control beams.

Measurements of optical tuning speed on W and Ka-Band oscillators confirmed tuning speeds in the nanosecond region. It was difficult to correlate the observed results with known oscillator circuit parameters, however the Ka-Band result of about 8ns was limited by the measurement system. Further experiments with oscillators of differing Q, operating at the same frequency, would be helpful.

In conclusion, optical tuning of IMPATT oscillators has been shown to be a practical technique at millimetre-wave frequencies. The first millimetre-wave IMPATT structure specially designed for optical control has been fabricated and demonstrated successfully. There remains a great deal of scope for further technology development based on the work presented in this report. Optically controlled IMPATT oscillators having the tuning performance achieved here would be useful in short range millimetre-wave communication links. Improvements in optical coupling efficiency should permit their use in phased-array radar and other large microwave systems, where the benefits of optical control signal distribution would be especially marked.

7.   References

[1]   J.F. Singleton, S. Brunt and A.J. Seeds, "Optically tuned mm-wave c.w. IMPATT source", Report TR85 on contract DAJA 45-84-C-0045, Marconi Electronic Devices Ltd., April 1986.

[2]   A.J. Seeds and J.R. Forrest, "Initial observations of optical injection locking of an X-Band IMPATT oscillator", Electron. Lett., 1978, 14, pp.829-830.

[3]   L. Picari and P. Spano, "New method for measuring ultrawide frequency response of optical detectors", Electron Lett., 1982, 18, pp.116-118.

[4]   W.T. Read, "A proposed high-frequency negative resistance diode", Bell Syst. Tech. J., 1958, 37, pp.401-446.

[5]   J.E. Carroll, Hot Electron Microwave Generators. London: Arnold, 1970, pp.197-212.

[6]   A.L. Cullen and J.R. Forrest, "Analytic theory of the IMPATT diode and its application to calculations of oscillator locking characteristics", Proc. IEE, 1974, 121, pp. 1467 - 1474.

[7]   A.J. Seeds and J.R. Forrest, "Initial observations of optical injection locking of an X-Band IMPATT oscillator", Electron. Lett., 1978, 14, pp. 829-830.

[8]   T. Misawa and N.D. Kenyon, "An oscillator circuit with cap structures for millimetre-wave IMPATT diodes", Trans. IEEE, 1970, MTT-18, pp. 969-970.

8.   Publications

[1]   J.F. Singleton, A.J. Seeds and S.P. Brunt, "Optical control of W-Band IMPATT oscillators", IEE Proc., 1986, 133J, pp. 349-352. (See Appendix C).

[2]   A.J. Seeds, J.F. Singleton, S.P. Brunt and J.R. Forrest: "The optical control of IMPATT oscillators", J. Lightwave Tech., 1987, LT-5, pp. 403-411. (see Appendix D).

9. Participating Personnel

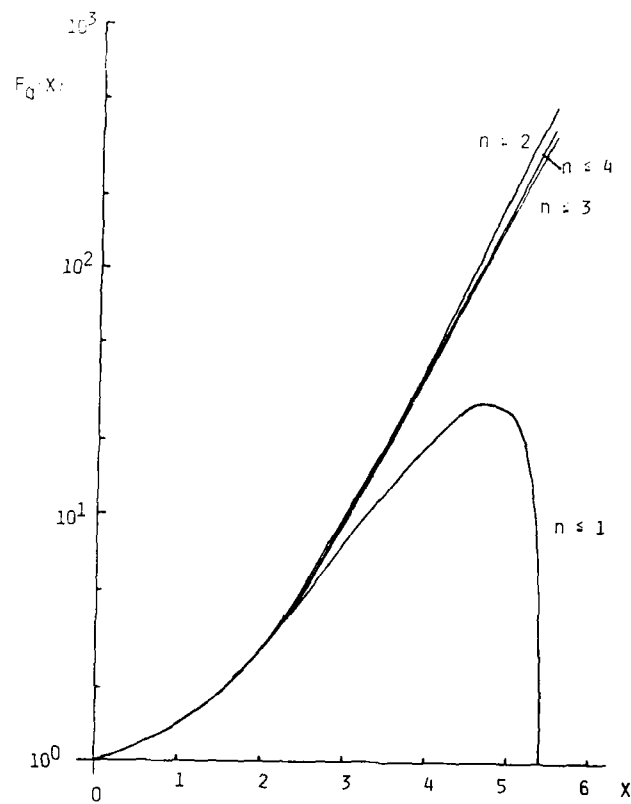| Dr. J.F. Singleton, | Marconi Electronic Devices Ltd., Lincoln. |
Miss S.P. Brunt,	" " " " "
Mr. I. Dale	" " " " "
Miss J. Taylor	" " " " "
Mr. D.A. Williams	" " " " "
Dr. J. Ondria	" " " " "
Dr. A.J. Seeds	Dept. of Electronic and Electrical Eng., University College London (Consultant)

Figure Captions

Figure 1a   Variation in avalanche gain coefficient $F_a\{X\}$ with voltage
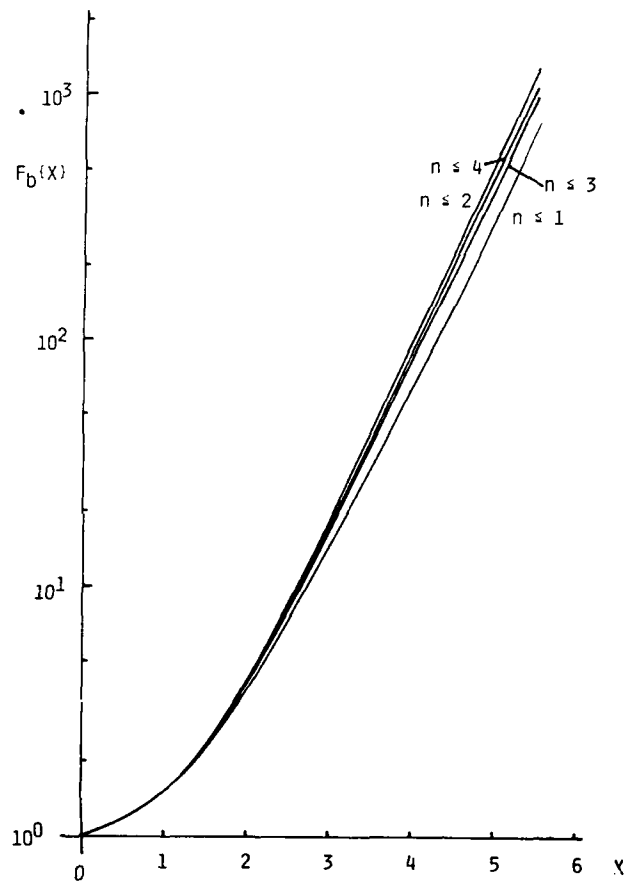   swing parameter X.

Figure 1b   Variation in avalanche gain coefficient $F_b\{X\}$ with voltage
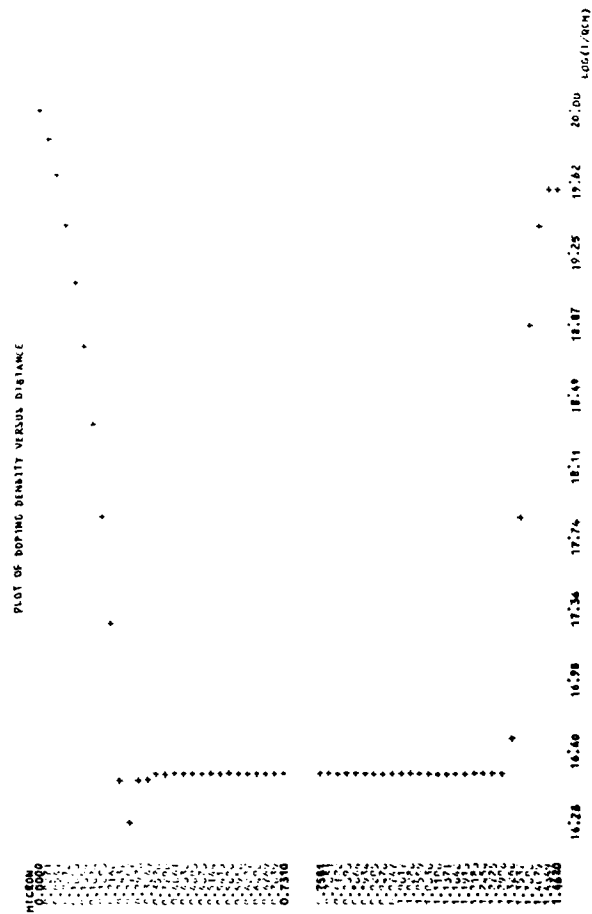   swing parameter X.

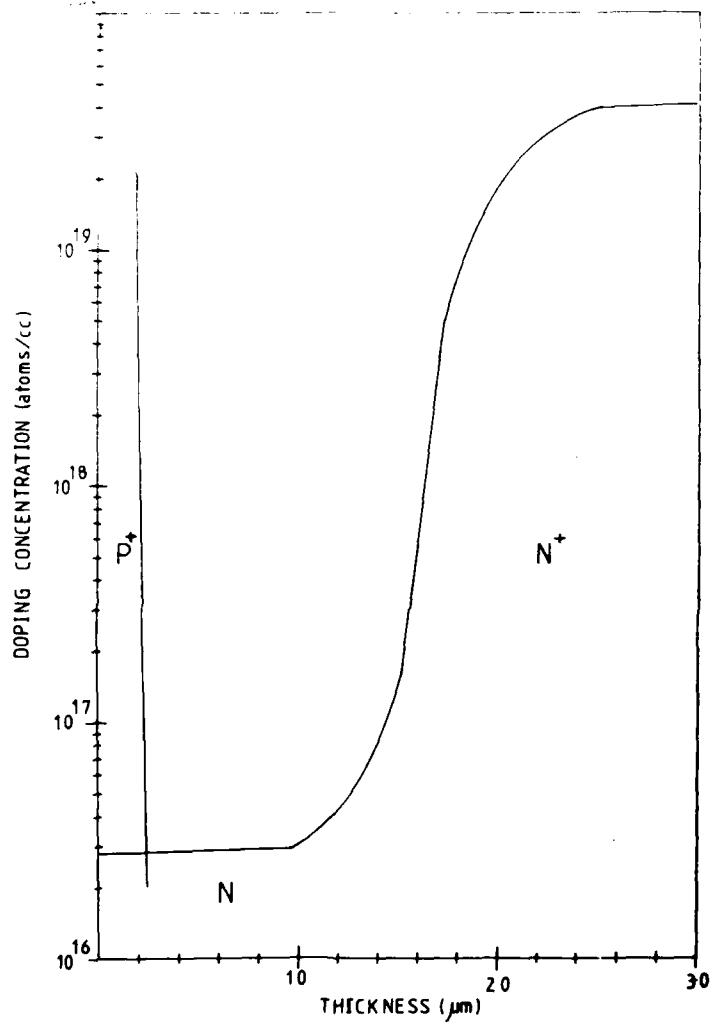Figure 2   Modelled doping profile of Ka-Band IMPATT structure.

Figure 3   Measured doping profile of Ka-Band IMPATT structure.
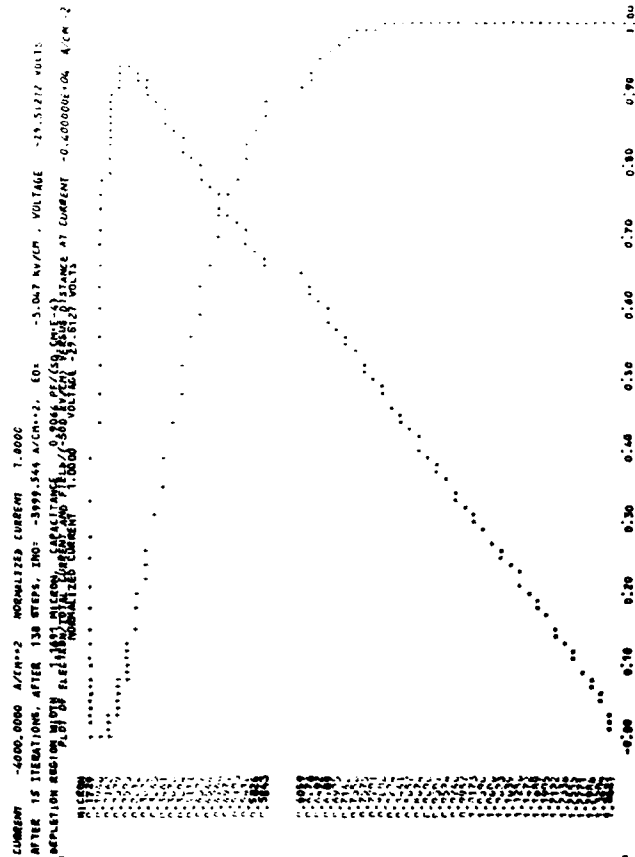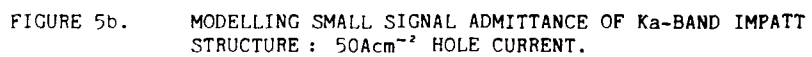
Figure 4   Modelled electric field and electron current density profiles for
             Ka-Band IMPATT diode.

Figure 5a   Modelled small signal admittance of Ka-Band IMPATT structure:
             unilluminated diode.

Figure 5b   Modelled small signal admittance of Ka-Band IMPATT structure:
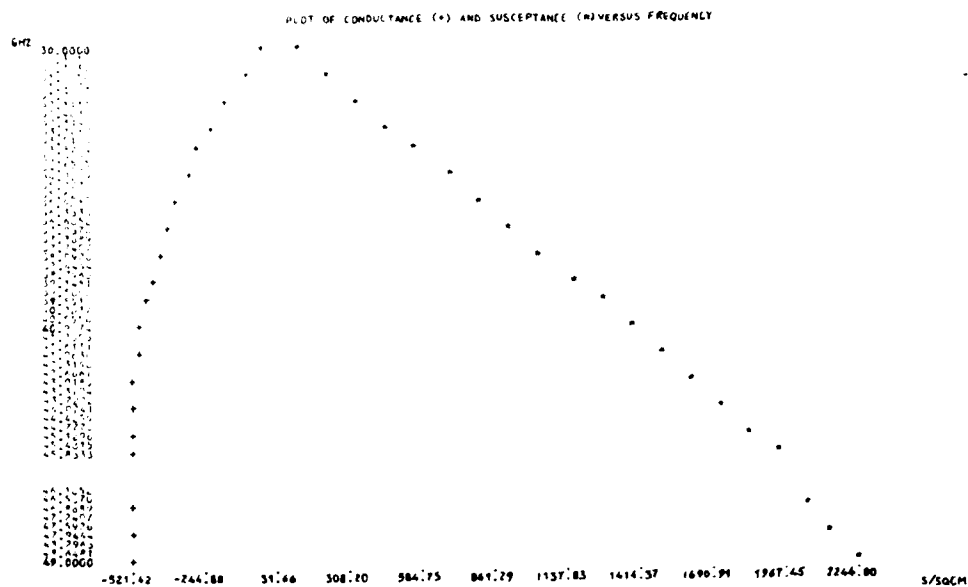   50 A cm^{-2} hole current.

Figure 5c   Modelled small signal admittance of Ka-Band IMPATT structure:
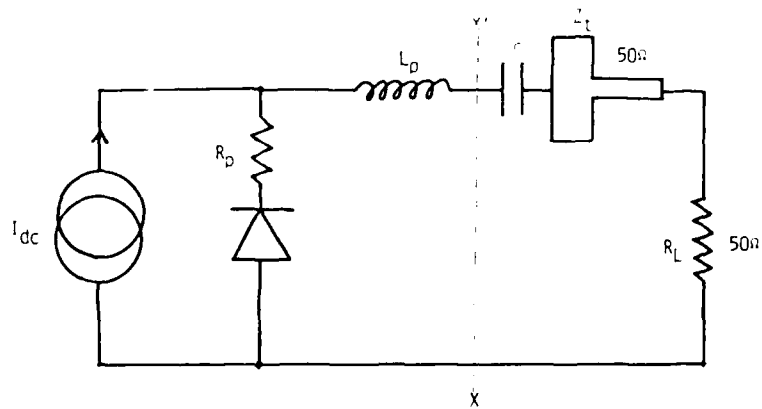   50 A cm^{-2} electron current.

Figure 6a   High Q circuit model for IMPATT oscillator optical tuning
             studies.

Figure 6b   Low Q circuit model for IMPATT oscillator optical tuning studies.

Figure 7   Optical tuning characteristics of low Q and high Q oscillator
             circuits.

Figure 8   Optical tuning transients for low Q oscillator circuit.

Figure 22   Etching of optical fibre. Transition from 125μm diameter fibre
to 70μm diameter etched fibre. (x 60 magnification).

FIGURE 1a. VARIATION IN AVALANCHE GAIN COEFFICIENT
$F_a\{X\}$ WITH VOLTAGE SWING PARAMETER X.

FIGURE 1b.   VARIATION IN AVALANCHE GAIN COEFFICIENT
$F_b\{X\}$ WITH VOLTAGE SWING PARAMETER X.

FIGURE 2.   MODELLING DOPING PROFILE OF Ka-BAND IMPATT STRUCTURE

FIGURE 3.   MEASURED DOPING PROFILE OF Ka-BAND IMPATT STRUCTURE

FIGURE 4. MODELLED ELECTRIC FIELD AND ELECTRON CURRENT DENSITY
PROFILES FOR Ka-BAND IMPATT DIODE.

PLOT OF CONDUCTANCE (+) AND SUSCEPTANCE (R) VERSUS FREQUENCY

FIGURE 5a.   MODELLING SMALL SIGNAL ADMITTANCE OF Ka-BAND IMPATT
              STRUCTURE:
              UNILLUMINATED DIODE

PLOT OF CONDUCTANCE (+) AND SUSCEPTANCE (*)VERSUS FREQUENCY

GHZ

-576.44   -290.95   -5.45   280.04   565.53   851.02   1136.51   1422.00   1707.49   1992.98   2278.47

S/SQCM

FIGURE 5b.   MODELLING SMALL SIGNAL ADMITTANCE OF Ka-BAND IMPATT
STRUCTURE : 50Acm⁻² HOLE CURRENT.

PLOT OF CONDUCTANCE (+) AND SUSCEPTANCE (R) VERSUS FREQUENCY

GHZ 30.0000

-921.42 -244.88 31.66 308.20 584.75 861.29 1137.83 1414.37 1690.91 1967.45 2244.00   S/SQCM

FIGURE 5c.   MODELLING SMALL SIGNAL ADMITTANCE OF Ka-BAND IMPATT STRUCTURE:
50Acm^{-2} ELECTRON CURRENT.

FIGURE 6a.   HIGH Q CIRCUIT MODEL FOR IMPATT OSCILLATOR
OPTICAL TUNING STUDIES.
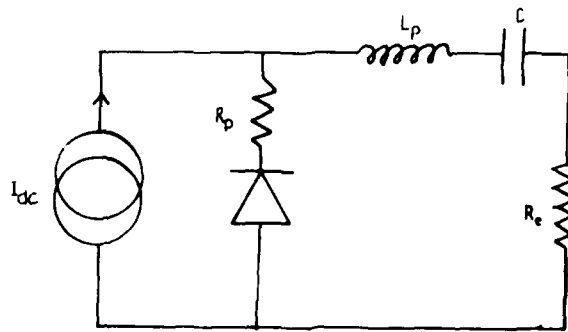
FIGURE 6b. LOW Q CIRCUIT MODEL FOR IMPATT OSCILLATOR OPTICAL TUNING STUDIES.
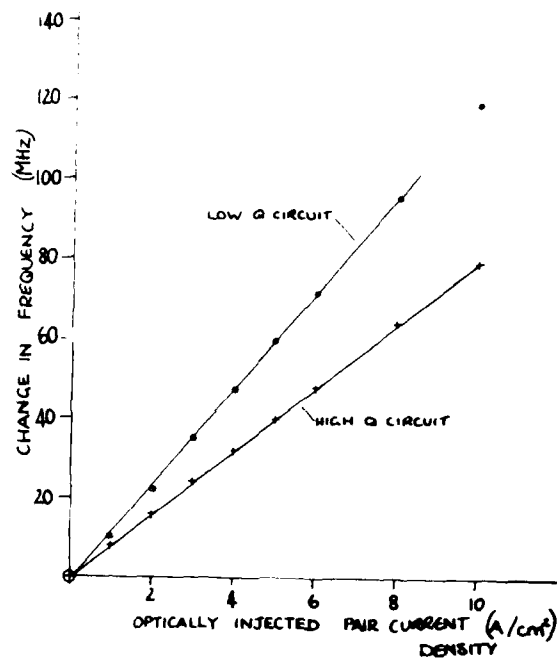
FIGURE 7. OPTICAL TUNING CHARACTERISTICS OF LOW Q AND HIGH Q
OSCILLATOR CIRCUITS.
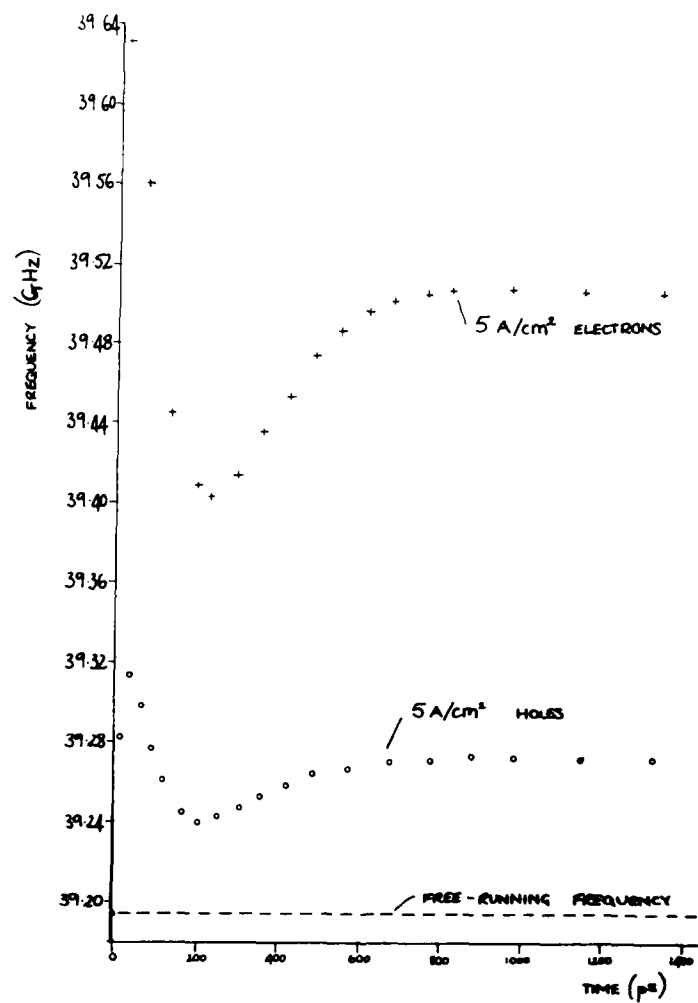
FIGURE 8.   OPTICAL TUNING TRANSIENTS FOR LOW Q OSCILLATOR CIRCUIT.
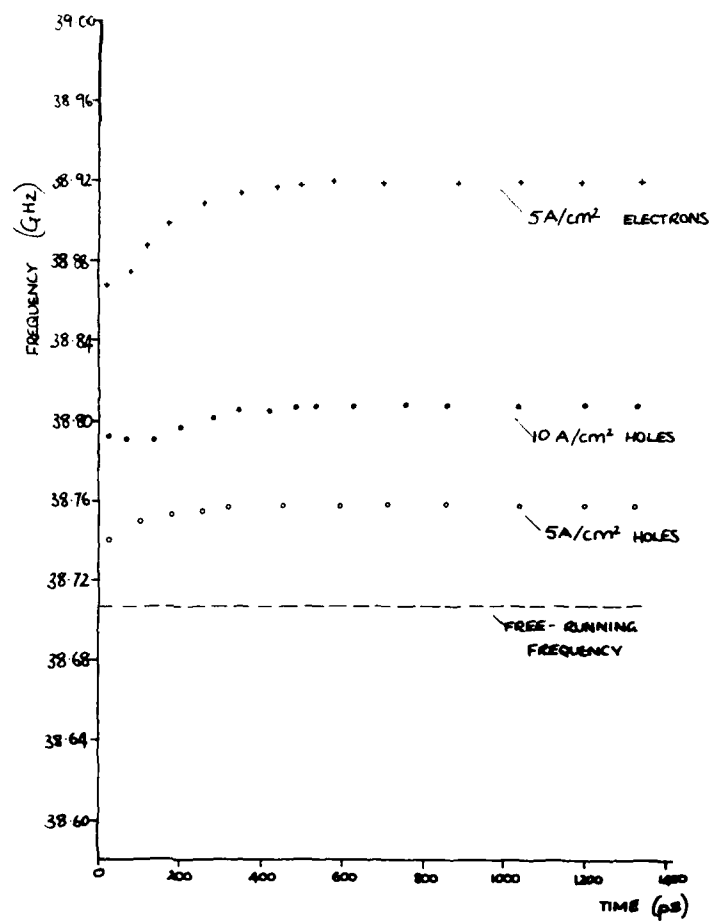
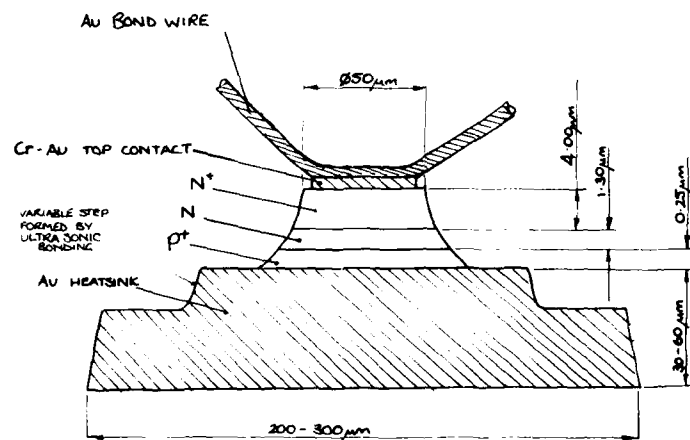FIGURE 9.   OPTICAL TUNING TRANSIENTS FOR HIGH Q OSCILLATOR CIRCUIT.

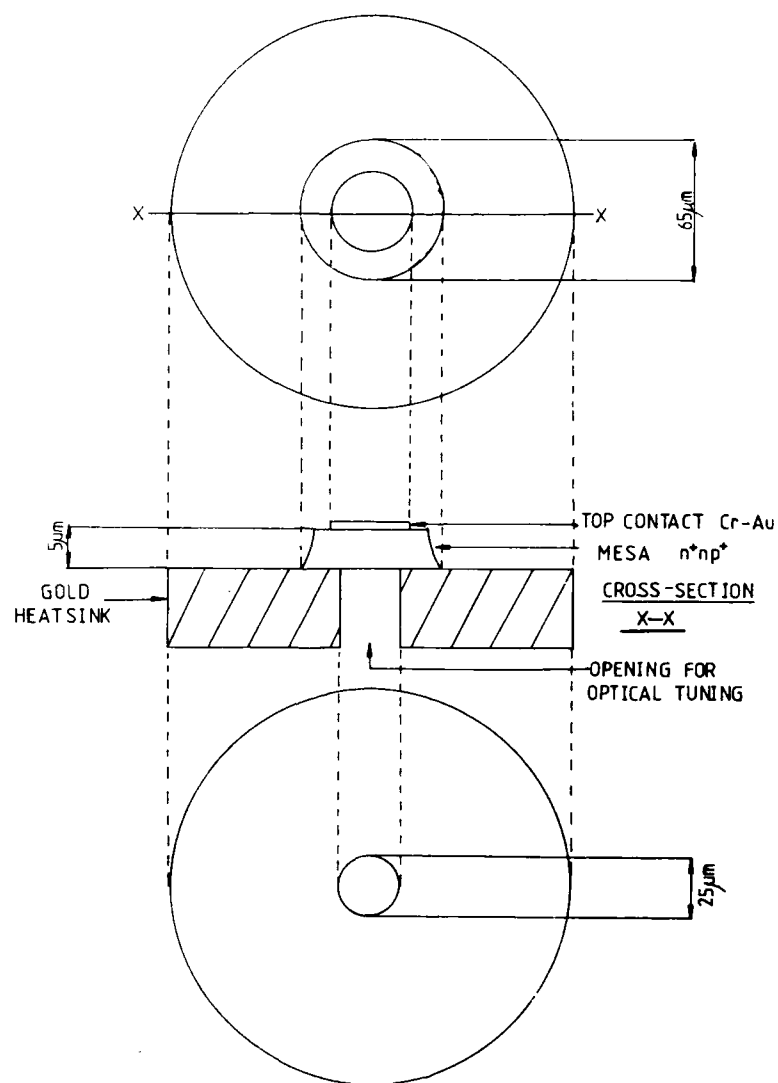FIGURE 10.   CROSS SECTION OF Ka-BAND IMPATT STRUCTURE.

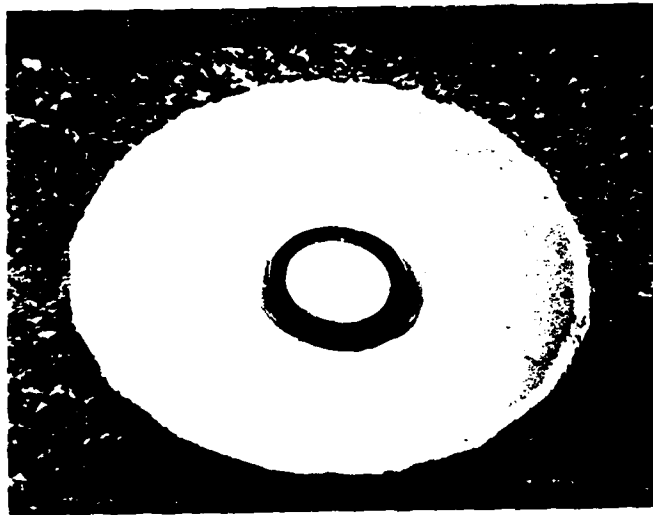FIGURE 11.   DRAWING OF Ka-BAND IMPATT STRUCTURE.

FIGURE 12.   TOP VIEW OF MODIFIED Ka-BAND IMPATT STRUCTURE.

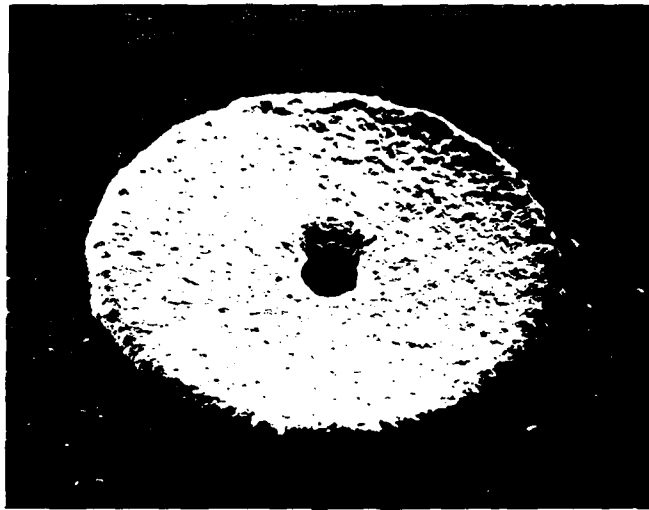FIGURE 13.   SIDE VIEW OF MODIFIED Ka-BAND IMPATT STRUCTURE.

FIGURE 14.   BOTTOM VIEW OF MODIFIED Ka-BAND IMPATT STRUCTURE
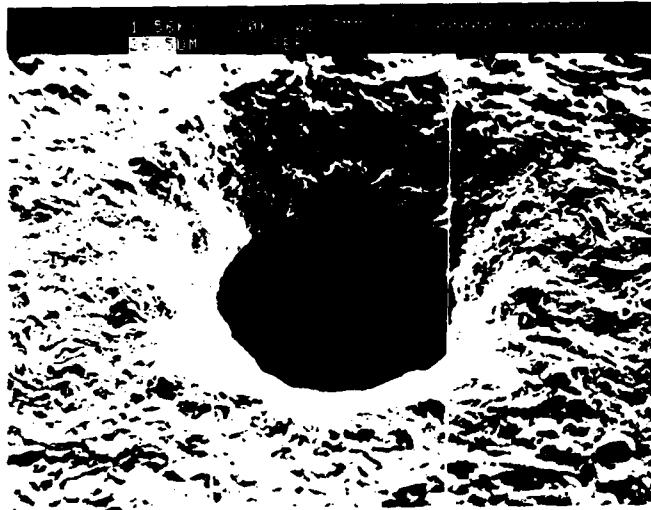   SHOWING HOLE FOR ILLUMINATION OF P^+ REGION.
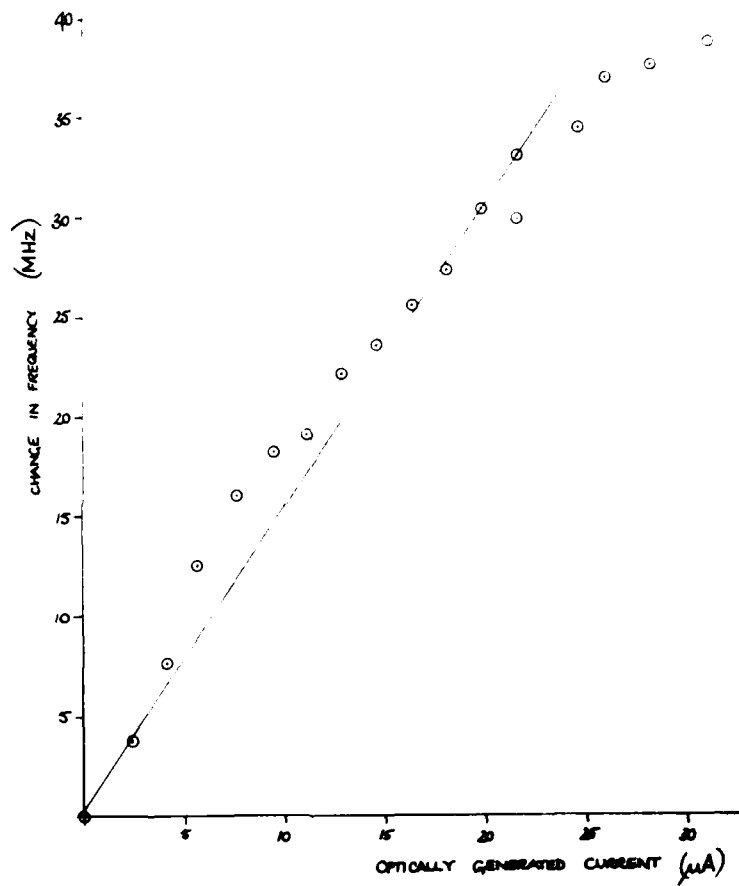
FIGURE 15.   DETAIL OF HEATSINK AND HOLE.

FIGURE 16.   OPTICAL TUNING CHARACTERISTIC OF Ka-BAND IMPATT
OSCILLATOR WITH EDGE ILLUMINATION.
(I_{dc} = 81mA, f_O = 38.4GHz)

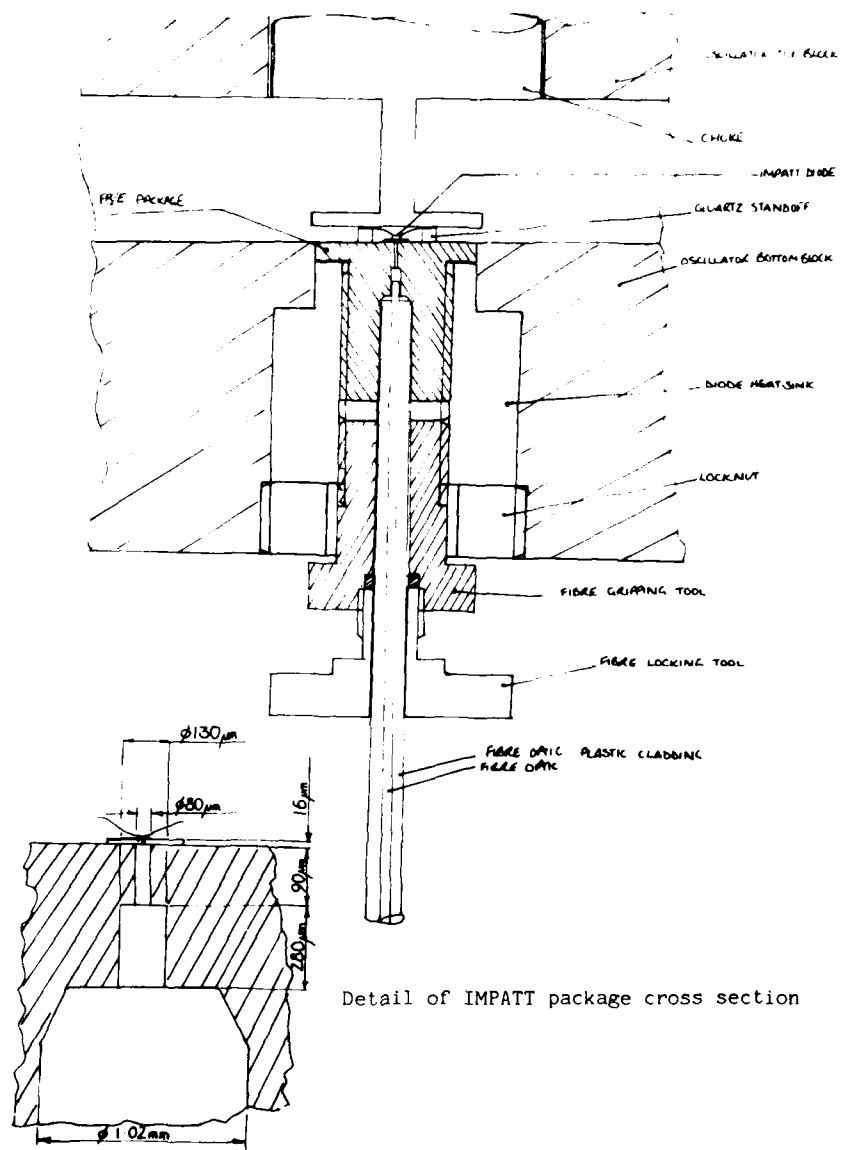Detail of IMPATT package cross section

FIGURE 17.   MOUNT FOR BASE ILLUMINATION OF MODIFIED IMPATT STRUCTURE.
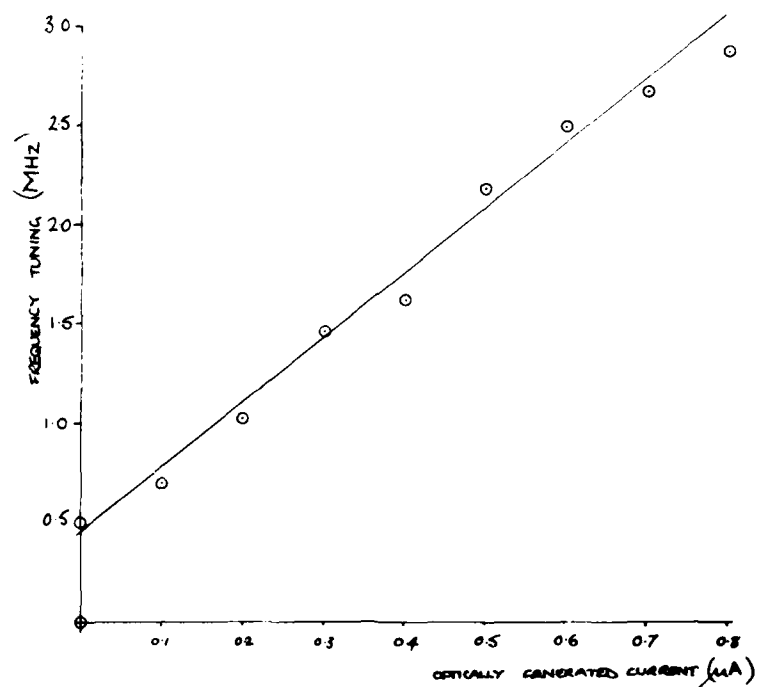
FIGURE 18. OPTICAL TUNING CHARACTERISTIC OF MODIFIED Ka-BAND
IMPATT STRUCTURE WITH BASE ILLUMINATION.
(I_{dc} = 49mA, f_O = 42GHz)
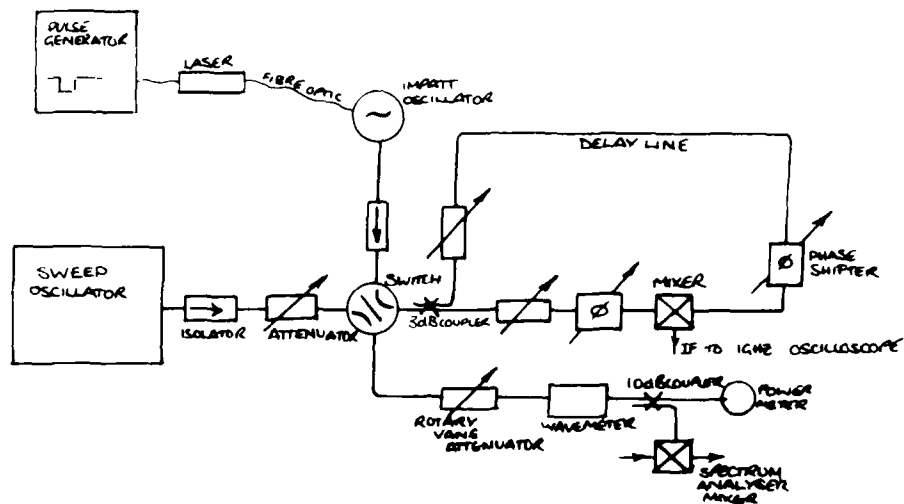
FIGURE 19. DELAY LINE DISCRIMINATOR SYSTEM USED FOR TUNING
SPEED MEASUREMENTS.

FIGURE 22. MEASUREMENT OF W-BAND OSCILLATOR TUNING SPEED.
UPPER TRACE: LASER BIAS PULSE. LOWER TRACE:
DISCRIMINATOR OUTPUT. HORIZONTAL SCALE 20ns DIV^{-1}.
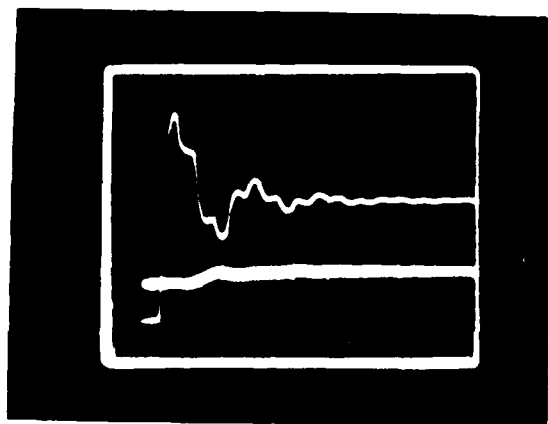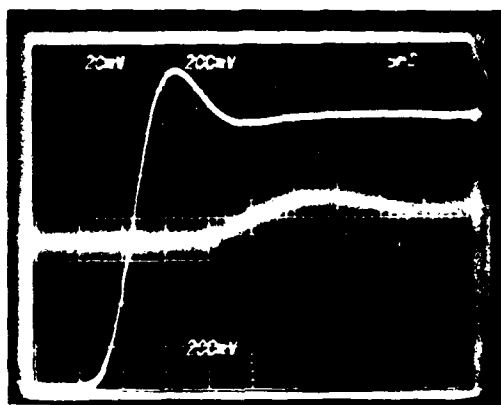
FIGURE 21.   MEASUREMENT OF Ka-BAND OSCILLATOR TUNING SPEED.
              UPPER TRACE: LASER BIAS PULSE. LOWER TRACE:
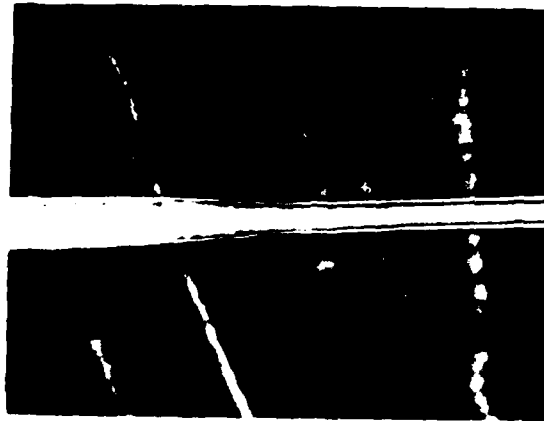   DISCRIMINATOR OUTPUT.
              HORIZONTAL SCALE 5ns DIV^{-1}.

FIGURE 22.   ETCHING OF OPTICAL FIBRE.   TRANSITION FROM 125µm
              DIAMETER FIBRE TO 70µm DIAMETER ETCHED FIBRE.
              (X 60 MAGNIFICATION).

General Analytic Theory of Optical Control

The theory of optical tuning presented previously [1] used truncated Bessel function series to estimate the optical tuning capabilities of IMPATT oscillators. As the voltage swing across the diode increases higher order Bessel function coefficients become significant and the model becomes less accurate. In this section more general expressions are developed which allow greater accuracy to be obtained at higher voltage swings. Also, opportunity has been taken to develop the theory for optical injection locking of IMPATT oscillators.

In optical injection locking the optical control signal is intensity modulated at a frequency close to the free-running frequency of the oscillator. This enables the oscillator frequency to be locked to the modulation frequency in a manner analogous to conventional electrical injection locking [2]. Whilst optical injection locking has yet to be demonstrated at millimetre-wave frequencies because of the technological difficulty in intensity modulating light at sufficiently high frequencies, recent developments in optical heterodyne technology [3] suggest that the technique may become of considerable systems interest in the future.

2.1 IMPATT Diode Model

A general analysis of the optically controlled IMPATT oscillator is made difficult by the extreme non-linearity of the avalanche multiplication process. However, if it is assumed that all carrier motion is at saturated velocity, v_s, and that electrons and holes have equal ionisation coefficients, α, a simple expression for the avalanche current density, J, can be written [4]:

$$\frac{\tau_a}{2} \frac{dJ}{dt} = J \left[\int_0^{L_a} \alpha \, dz - 1 \right] + J_s \tag{1}$$

where L_a is the avalanche zone length, τ_a $(= L_a/v_s)$ is the avalanche zone transit time and J_s is the total reverse saturation current density including both optically and thermally generated components:

$$J_s = J_{so} + J_{s1} \sin(\omega t + \phi) \tag{2}$$

Here J_{so} is the constant thermally and optically generated saturation current and J_{s1} is the peak value of an optically generated locking current of frequency ω and arbitrary phase constant ϕ.

To solve equation (1) an expression for the electric field dependence of the ionisation coefficient, α, is required. A useful model is

$$\alpha = \alpha_o \left(\frac{E}{E_o} \right)^m \tag{3}$$

where E is the electric field, m is an ionisation non-linearity constant ($m \approx 6$ for silicon) and α_o and E_o are constants. Assuming that the avalanche zone is uniformly doped, that the field in the drift zone is much less than the peak field within the diode and that the voltage swing across the diode is moderate, then, following Carroll [5], the ionisation integral in equation (1) can be

evaluated to give

$$\frac{d\,J}{d\,t} = \frac{2(m+1)}{\tau_a}\,J\left[\frac{m}{4}\left(\frac{E_1}{E_{po}}\right)^2 - \frac{E_b}{E_{po}} + \frac{E_1}{E_{po}}\,\sin(\omega t + \delta)\right] + \frac{2\,J_s}{\tau_a}$$

(4)

where harmonic terms are neglected and the peak electric field, E_p, is represented by

$$E_p = E_{po} - E_b + E_1\,\sin(\omega t + \delta)$$

(5)

for a diode terminal voltage

$$v = V_{po} + L(E_1\,\sin(\omega t) - E_b)$$

(6)

Here E_b is a back bias field resulting from the combined effects of ionisation non-linearity, reverse saturation current and carrier space charge, E_1 is the peak value of the modulated component of electric field, L is the total depletion width and V_{po} the breakdown voltage. Equation (6) assumes the diode to be embedded in an oscillator circuit of moderately high Q factor, so that the voltage variation will be nearly sinusoidal, and that the diode remains punched-through over the whole r.f. cycle. It is also assumed that the oscillator is locked to the incident modulated optical signal, where present, to give an oscillation frequency of ω. The injection locking range can then be found from the limiting conditions on the phase angle, ϕ. The phase angle, δ, is used to represent back bias and carrier space charge effects: details of its evaluation are given by Cullen and Forrest [6].

Equation (4) is a linear, first order equation, and can be solved using an integrating factor expanded in terms of modified Bessel functions. Following integration across the drift zone the fundamental component of the device external conduction current can be written

$$
J_1 = \frac{\sin\left(\frac{\omega \tau_d}{2}\right)}{\left(\frac{\omega \tau_d}{2}\right)} \left[\begin{array}{l} - 2 J_{dc} \frac{I_1\{X\}}{I_0\{X\}} \cos(\omega(t - \frac{\tau_d}{2}) + \delta) \\[2em] + 4 J_{so}\left[\frac{I_0\{X\} I_1\{X\}}{\omega \tau_a} \right. \\[1.5em] \left. + \sum_{n=1}^{\infty} \frac{(-1)^n (2n+1) I_{n+1}\{X\} I_n\{X\}}{n(n+1) \omega \tau_a} \right] \\[1.5em] \cdot \sin(\omega(t - \frac{\tau_d}{2}) + \delta) \\[2em] - J_{s1}\left[\frac{2 I_0^2\{X\} - I_1^2\{X\} - I_1\{X\} I_3\{X\}}{\omega \tau_a} \right. \\[1.5em] \left. - 4 \sum_{n=2}^{\infty} \frac{(-1)^n I_n^2\{X\}}{(n-1)(n+1) \omega \tau_a} \right] \\[1.5em] \cdot \cos(\omega(t - \frac{\tau_d}{2}) + \phi) \end{array} \right]
$$

(7)

where τ_d is the drift zone transit time and $I_n\{X\}$ are modified Bessel function coefficients of order n and argument

$$
X = \frac{2(m+1) E_1}{\omega \tau_a E_{po}}
$$

(8)

In deriving equation (7) it has been assumed that $J_{s1} \ll J_{so} \ll J_{dc}$ so that the effect of the optically injected current on the diode bias voltage is small.

Equation (7) contains three clearly identifiable terms; the term in $\cos(\omega t + \delta)$ represents the fundamental component of the main avalanche current, that in $\sin(\omega t + \delta)$ a quadrature term that alters the phasing of the avalanche current in response to reverse saturation current J_{so}, while the term in $\cos(\omega t + \phi)$ represents the optical injection locking signal. The first two terms can be combined by introducing a modified phase angle, δ_s:

$$\delta_s = \delta + \sin^{-1}\left(2 \frac{J_{so}}{J_{dc}\ \omega\ \tau_a} F_a\{X\}\right) \tag{9}$$

where the avalanche gain factor for optical tuning, $F_a\{X\}$, is defined by

$$F_a\{X\} = I_0^2\{X\} + \frac{I_0\{X\}}{I_1\{X\}} \sum_{n=1}^{\infty} \frac{(-1)^n (2n+1) I_{n+1}\{X\} I_n\{X\}}{n(n+1)} \tag{10}$$

Equation (7) can then be rewritten

$$J_1 = -2 J_{dc} \frac{\sin\left(\dfrac{\omega \tau_d}{2}\right)}{\left(\dfrac{\omega \tau_d}{2}\right)} \frac{I_1\{X\}}{I_0\{X\}} \cos(\omega(t - \frac{\tau_d}{2}) + \delta_s)$$

$$- \frac{2 J_{s1}}{\omega \tau_a} \frac{\sin\left(\dfrac{\omega \tau_d}{2}\right)}{\left(\dfrac{\omega \tau_d}{2}\right)} F_b\{X\} \cos(\omega(t - \frac{\tau_d}{2}) + \phi)$$

$$\tag{11}$$

where $F_b\{X\}$ is an avalanche gain factor for optical injection locking:

$$F_b\{X\} = I_0^2\{X\} - \frac{I_1^2\{X\} + I_1\{X\} I_3\{X\}}{2} - 2 \sum_{n=2}^{\infty} \frac{(-1)^n I_n^2\{X\}}{(n-1)(n+1)} \tag{12}$$

Equations (9) to (12) represent a generalisation of the earlier analysis [1] and enable predictions of optical tuning and injection locking performance to be made when coupled with a suitable oscillator circuit model.

The avalanche gain factors defined by equations (10) and (12) are strong functions of the peak r.f. voltage swing across the IMPATT diode through the Bessel function argument dependence on peak modulated electric field, equation (8). In evaluating these gain factors the number of terms in the Bessel function series that need to be taken into account depends on the argument value, X. A typical IMPATT might have

$$\tau_a = 0.2 \ \tau_d = 0.2 \ \pi/\omega_o \qquad\qquad (13)$$

where ω_o is the free running oscillator frequency. Thus, for $\omega = \omega_o$, $m = 6$ and a maximum voltage modulation of 25%, $X \leq 5.6$. Figure 1 shows the variation in $F_a\{X\}$ and $F_b\{X\}$ with X for $n \leq 1$ to 4. It can be seen that truncating the series at $n = 3$ provides sufficient accuracy for most purposes.

For $X = 4.5$, corresponding to about 20% voltage modulation $F_a\{X\} = 78$ and $F_b\{X\} = 209$ showing that avalanche gain enhances the optical control sensitivity considerably.

2.2 Oscillator Circuit Model

To obtain predictions of the optical tuning and locking ranges a circuit model for the oscillator is required. Figure A.1 shows a simple lumped model in which the IMPATT is represented by an admittance Y_1 ($= G_1 + j \ B_1$) and the load by a parallel LR circuit of admittance Y_L ($= G_L + j \ B_L$). The optical injection locking signal is represented by a current generator, i_ℓ, defined from equation (11) as

$$i_\ell = - \frac{2 \ J_{s1} \ A \ F_b\{X\}}{\omega \ \tau_a} \ \frac{\sin\left(\dfrac{\omega \ \tau_d}{2}\right)}{\left(\dfrac{\omega \ \tau_d}{2}\right)} \ \exp \ j\left(\omega\left(t - \frac{\tau_d}{2}\right) + \phi\right) \qquad (14)$$

where A is the diode area. From equation (6) the r.f. voltage across the diode

is given by

$$v_1 = - j \ V_1 \ \exp j(\omega \ t) \tag{15}$$

where $V_1 = E_1 \ L$. Thus the circuit equation for Figure A.1

$$i_\ell = (Y_1 + Y_L) \ v_1 \tag{16}$$

2.3 Optical Tuning Predictions

If there is no injected locking signal G_L and B_L are obtained from equations (11), (15) and (16), setting $J_{s1} = 0$ and adding the diode depletion susceptance, $\omega \ C_d$, to the active susceptance:

$$G_L = \frac{4 \ I_{dc} \ \sin\left(\frac{\omega \ \tau_d}{2}\right) \ I_1\{X\}}{V_1 \ \omega \ \tau_d \ I_0\{X\}} \ \sin \ (\frac{\omega \ \tau_d}{2} - \delta_s) \tag{17}$$

$$B_L = \frac{4 \ I_{dc} \ \sin\left(\frac{\omega \ \tau_d}{2}\right) \ I_1\{X\}}{V_1 \ \omega \ \tau_d \ I_0\{X\}} \ \cos \ (\frac{\omega \ \tau_d}{2} - \delta_s) - \omega \ C_d \tag{18}$$

where $I_{dc} = J_{dc} \ A$. Dividing equation (18) by equation (17) and defining B_L as $B_L = - 1/(\omega \ L_L)$ gives

$$\omega \ C_d - \frac{1}{\omega \ L_L} = G_L \ \cot \ (\frac{\omega \ \tau_d}{2} - \delta_s) \tag{19}$$

The tuning sensitivity can be obtained by assuming that $\omega = \omega_0 + \Delta\omega$, where $\omega_0 = (L_L \ C_d)^{-0.5}$. Then for $\delta_s \ll \pi/2$ substitution of equation (9) in equation (19) with assumption (13) yields

$$\Delta\omega = \frac{G_L}{2 \ C_d} \left[\delta + 2 \ \frac{I_{so} \ F_a\{X\}}{I_{dc} \ \omega_0 \ \tau_a} \right] \tag{20}$$

where $I_{so} = J_{so} \ A$. The optical frequency tuning slope is then

$$\frac{d\,(\Delta\omega)}{d\,I_{so}} = \frac{G_L\,F_a\{X\}}{C_d\,I_{dc}\,\omega_o\,\tau_a} \tag{21}$$

Defining oscillator Q factor as

$$Q = \frac{\omega_o\,C_d}{G_L} \tag{22}$$

equation (21) can be rewritten

$$\frac{d\,(\Delta\omega)}{d\,I_{so}} = \frac{F_a\{X\}}{Q\,I_{dc}\,\tau_a} \tag{23}$$

This shows that the optical tuning slope is proportional to the avalanche gain factor, $F_a\{X\}$, and inversely proportional to the oscillator Q. Comparison of equation (23) with the corresponding equation in [1], equation (4.26), shows that the only difference lies in the definition of the factor $F_a\{X\}$. That defined by equation (4.27) of [1] incorporates only the first term of equation (10). Reference to Figure 1a shows that this introduces a serious error for a voltage swing parameter, X, greater than 4, whereas the inclusion of an extra one or two terms gives good accuracy up to the largest voltage swings likely to be encountered in practice.

2.4 Optical Injection Locking Predictions

In optical injection locking $i_\ell \neq 0$. Substituting equations (14), (15), (17) and (18) in equation (16), with the assumption (13) and for $\delta_s \ll \pi/2$, gives the real part of equation (16) as

$$\frac{4\,I_{s1}\,F_b\{X\}}{\pi\,\omega_o\,\tau_a\,V_1}\sin\phi = \omega\,C_d - \frac{1}{\omega\,L_L} \tag{24}$$

where $I_{s1} = J_{s1}\,A$.

Applying the Adler [2] condition, $\sin\phi = \pm\,1$, the locking range is found

to be

$$2 \Delta\omega_L \quad \frac{4 \ I_{s1} \ F_b \ \{X\}}{\pi \ \omega_o \ \tau_a \ v_1 \ C_d} \qquad (25)$$

This can be restated in a form similar to the Adler locking equation by substituting from equation (22) with equation (17) and assumption (13):

$$2\Delta\omega_L = 5 \ F_b\{X\} \ \frac{I_0\{X\}\omega_c \ I_{s1}}{I_1\{X\} \ Q \ I_{dc}} \qquad (26)$$

Thus the locking range is proportional to the optically injected current I_{s1} and the avalanche gain factor $F_b\{X\}$, and inversely proportional to the oscillator Q.

An estimate of the locking range likely to be achieved in practice can be made using data from the W-Band IMPATT oscillator used in previous experimental work [1]. This had a Q of 200 and an operating frequency of about 94 GHz with a bias current of 100mA. The voltage swing parameter, X, was approximately 3.5, giving $F_b\{X\}$ = 40 from Figure 1b. Substituting these values in equation (26) gives a locking range dependence on injected modulated current of 1.09GHz mA^{-1}, or a locking range of about 22MHz for the illumination configuration used in [1]. Previous work on X-Band oscillators [7] gave measured locking ranges of a few megahertz, which would accord with the predictions of equation (26) if differences in Q and operating frequency are taken into account. It should be noted that equation (26) takes no account of locking stability. This can be treated using the methods described in [6].

Figure A.1: Equivalent circuit for optically controlled IMPATT oscillator.
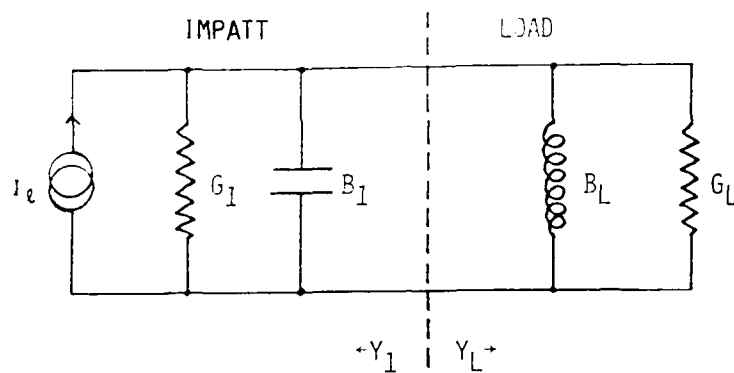
FIGURE A1.   EQUIVALENT CIRCUIT FOR OPTICALLY CONTROLLED
             IMPATT OSCILLATOR.

Appendix B. The Quarter Wave Transformer.

The analysis starts from the equation for the input impedance of an arbitrarily terminated length of transmission line

$$Z_i = Z_t \left[\frac{Z_L \cos \beta\ell + jZ_t \sin \beta\ell}{Z_t \cos \beta\ell + jZ_L \sin \beta\ell} \right] \qquad \ldots\ldots\ldots(1)$$

where Z_t is the characteristic impedance of the line, Z_L the impedance of the load and ℓ the length of the line. The propagation constant, β, is defined by

$$\beta = \frac{\omega}{c} = \frac{2\pi}{\lambda} \qquad \ldots\ldots\ldots(2)$$

where λ is the wavelength. In the quarter wave transformer $\ell = \lambda/4$ and equation 1 reduces to

$$Z_i = \frac{Z_t^2}{Z_L} \qquad \ldots\ldots\ldots(3)$$

For oscillator matching transformers $Z_t \ll Z_L$. Rationalising equation A.3.2.1 and neglecting terms in Z_t^2 relative to those in Z_L^2 gives

$$Z_i \approx \frac{Z_t^2}{Z_L \sin^2 \beta\ell} - j Z_t \cot\beta\ell \qquad \ldots\ldots\ldots(4)$$
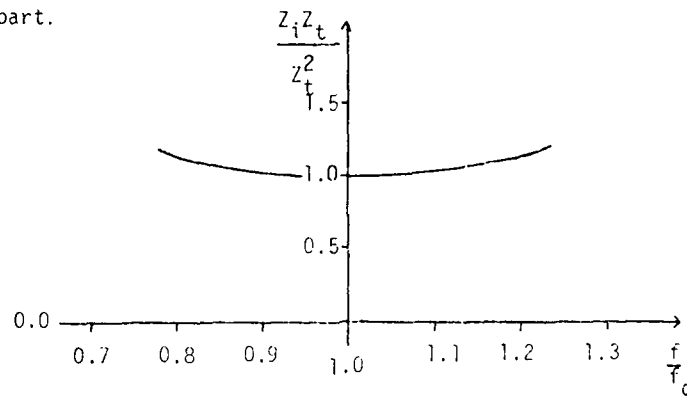
With $Z_t = Z_L/5$, and at a frequency within 20% of the resonant frequency of the transformer, the error introduced by equation 4.

is less than 0.4%. From equation 2.

$$\beta \ell = \frac{\pi f}{2 f_0}$$

....

where f_0 is the frequency at which $\ell = \lambda/4$. Figure B.1 is a plot of the real and imaginary parts of equation 4 as a function of frequency.
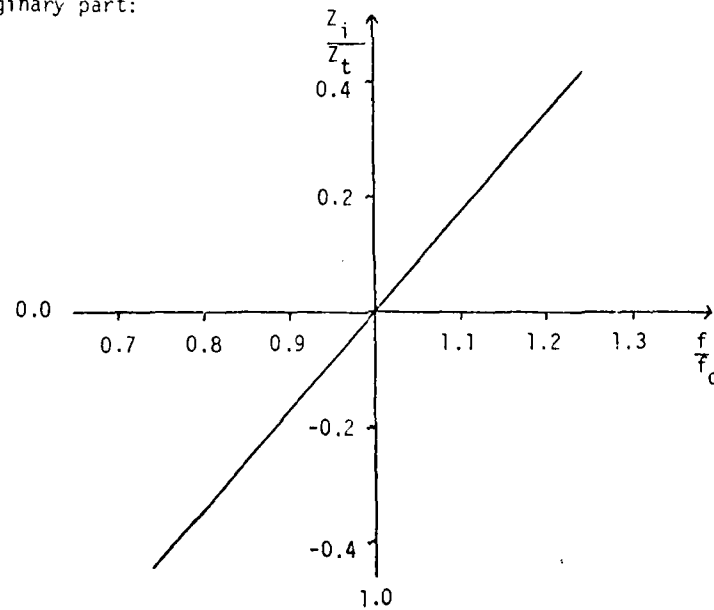
Real part.

Imaginary part:

Figure B.1   Plot of input impedance of quarter wave transformer against frequency.

Where $\phi \ell \approx \pi/2$ equation 4 can be rewritten as

$$Z_i \approx Z_t^2 - j \frac{Z_t \pi}{2} \left(1 - \frac{f}{f_0} \right) \qquad \dots\dots\dots(4a)$$

The quarter wave transformer and load can then be represented by the series resonant circuit of Figure B.2
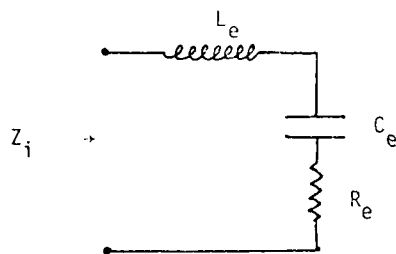

Fig. B.2   Series equivalent circuit for quarter wave transformer near to resonance.

For Figure B.2

$$Z_i = R_e + j \left(\omega L_e - \frac{1}{\omega C_e} \right) \qquad \dots\dots\dots(6)$$

Close to series resonance equation 6 can be rewritten as

$$Z_i \approx R_e - j \, 4\pi \, f_0 L_e \left(1 - \frac{f}{f_0} \right) \qquad \dots\dots\dots(7)$$

Comparison with equation 4a gives the values of the equivalent

circuit components as

$$R_e = \frac{Z_t^2}{Z_L} \qquad \dots\dots(8)$$

$$L_e = \frac{Z_t}{8f_o} \qquad \dots\dots(9)$$

and, from the resonance condition

$$C_e = \frac{2}{\pi^2 f_o Z_t} \qquad \dots\dots(10)$$

APPENDIX C

Optical control of W-band impatt oscillators

J.F. Singleton, A.J. Seeds and S.P. Brunt

Abstract: Results are presented for analytical computer modelling and experimental studies of optically induced frequency tuning of W-Band (75–110 GHz) impatt oscillators. Predictions from an analytical theory are compared with those from a large-signal time-domain computer model, and the effect of unequal electron and hole ionisation coefficients on the tuning performance is illustrated. Experimental measurements are presented showing an optical tuning range of about 10 MHz for an optically generated current of 20 µA, and comparisons are made with the theoretical predictions.

1 Introduction

The impatt diode is currently the only solid-state source capable of providing the transmitter power requirements in small, millimetre-wave radar systems. In many applications, particularly in FMCW radars, it is necessary to tune the transmitter frequency electronically, however such control of impatt diode oscillators is found to be very difficult to implement because of the power impedance levels involved.

Tuning of impatt oscillators in practical systems is normally achieved by using a varactor-controlled Gunn oscillator (VCO) to injection lock the impatt. This system works very well but has the disadvantage of an extra oscillator cavity which may cause problems where size and weight of the system are prime considerations.

A novel alternative approach is to use an optical signal to generate carriers in the impatt by the photo-electric effect. These carriers drift into the avalanche zone of the diode and alter the phasing of the avalanche cycle, thereby changing the oscillation frequency.

Optical frequency tuning effects have previously been observed in Trapatts [1], bipolar transistors [2] and MESFETS [3]. Early work on the optical tuning of impatts was carried out predominantly at X-Band frequencies [4, 5]. This paper reports work to extend the technique to W-Band (75–110 GHz).

2 Analytic theory of optical frequency tuning in impatt oscillators

The physical mechanism underlying optical frequency tuning is the generation of hole-electron pairs in the impatt by the incident light, with consequent alteration in the timing of the avalanche cycle. It is therefore possible to calculate the change in oscillation frequency using a modified Read [6] approach. Making the simplifying assumptions of equal carrier velocities and avalanche ionisation coefficients for holes and electrons, the total avalanche current is given by [6]

$$\frac{\tau_a}{2}\frac{dJ}{dt} = J\left[\int_0^{w_a} \alpha\, dz - 1\right] + J_s \qquad (1)$$

where J_s is the total reverse saturation current density including both thermal and optical carrier generation, α the avalanche ionisation coefficient, w_a the avalanche zone

width and τ_a the avalanche zone transit time. Integration of eqn. 1 using a power law approximation for the dependence of the ionisation coefficient on electric field, together with a transit-time model for the drift zone, enables the change in oscillator frequency for a small optically injected current, I_{so}, to be written as

$$\Delta f_o = \frac{F_a\{x\} I_{so}}{2\pi Q I_{dc} \tau_a} \qquad (2)$$

where I_{dc} is the diode bias current, Q the oscillator external Q-factor and $F_a\{x\}$ an avalanche gain factor defined by

$$F_a\{x\} = \frac{2I_o^2\{x\} - 3I_o\{x\}I_2\{x\}}{2} \qquad (3)$$

Here $I_n\{x\}$ are modified Bessel function coefficients of order n and argument

$$x = \frac{(m + 1)V_1}{\pi f_o \tau_a E_{po} w} \qquad (4)$$

where f_o is the oscillation frequency, V_1 the peak RF voltage across the diode, E_{po} the peak electric field at breakdown, w the total depletion width and m the ionisation non-linearity coefficient. $F_a\{x\}$ is a strong function of the RF voltage swing though the V_1 dependence of the Bessel function argument x. For simplicity, eqn. 3 neglects Bessel coefficients of order greater than 2, a reasonable approximation for small to moderate voltage swings ($x \leqslant 4$).

The relationship between the optically generated current and the incident optical power is dependent on the device structure and illumination geometry. Assuming that all of the light is absorbed within the depletion layer the optically generated current is given by

$$I_{so} = \frac{\eta_q e\lambda P_{op}}{hc} \qquad (5)$$

where P_{op} is the incident optical power, η_q the quantum efficiency, λ the optical wavelength, e the electronic charge, h Planck's constant and c the velocity of light in vacuo. For $\lambda = 850$ nm and $\eta_q = 0.9$, $I_{so}/P_{op} = 0.62$ A W^{-1}. In practice, difficulties in securing efficient coupling between the light source and the impatt lead to much smaller values.

3 Computer modelling studies

The analytical theory gives a very useful estimate of the magnitude of optical tuning effects, but it is limited in accuracy as a result of the assumption of equal ionisation

coefficients for electrons and holes and, in any case, cannot be used to study transient effects in devices.

A large-signal time-domain computer model of the optically controlled impatt has therefore been developed from the earlier avalanche diode modelling work of Blakey et al. [7] The model is based on the solution in one spatial dimension and time of the drift-diffusion approximation to Boltzmann's transport equation, the equations for electron and hole continuity, and Gauss' theorem within the semiconductor material of the device. This approach enables spatially varying optical carrier generation to be taken into account.

Modelling studies were performed for a W-Band, silicon, single drift structure having a doping profile similar to that of the devices used in the experimental work. A simple oscillator circuit, shown in Fig. 1, was
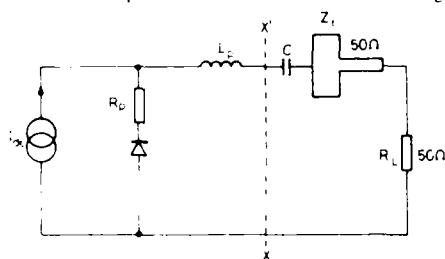

Fig. 1 *Oscillator equivalent circuit for modelling studies*

coupled to the diode to permit predictions of optical frequency tuning. L_p represents the diode bond wire inductance, R_p the diode parasitic resistance, R_L the load resistance, C the DC block capacitance and Z_t a quarter-wavelength transformer. If L_p is selected to resonate with the capacitive susceptance of the diode, then the impedance at plane X — X', looking towards the diode, is real and negative. The amplitude of the oscillation is then determined by selecting Z_t to match R_L to the impedance at X — X' for the required operating point. With values of 4 pF for C_p, 1 Ω for R_p, and a bias current of 140 mA, the model gave stable oscillation frequency of 94 GHz. The modelled efficiency was 3.6%, which is a typical value for a W-Band single-drift silicon device.

The computer model can also be used to study transient effects, and Fig. 2 shows the tuning transient resulting
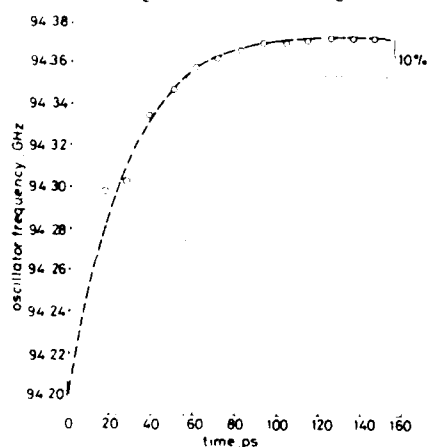

Fig. 2 *Impatt oscillator optical tuning transient for step change in illumination, I_p 0 to 2 A cm^2, I_{dc} 28.45 KA/cm^2, electron injection*

350

from a step change in optically injected electron current from 0 to 2 A cm^{-2}. It is seen that 90% of the frequency change was achieved in 55 ps, which compares very favourably with the speed of conventional electronic tuning techniques such as varactor tuning and may afford novel systems possibilities.

Two different optical carrier generation configurations were investigated in the study. In the first, electrons were injected into the depletion zone from the p$^+$ region, whereas in the second, holes were injected from the n$^+$ region. These correspond to illumination from opposite ends of the impatt structure. Fig. 3 shows the optical
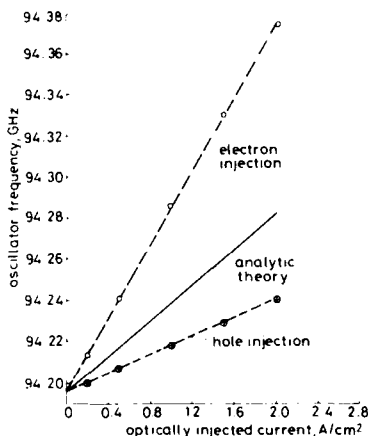

Fig. 3 *Comparison between computer model and analytic theory for optical tuning characteristics*
Bias current density 28.5 KA/cm^2

tuning characteristics obtained for optically injected current densities of up to 2 A/cm^2, corresponding to a current of 10 μA in the experimental diode. The change in frequency with injected current is seen to be linear, as predicted by eqn. 2. A more detailed comparison with the analytic theory can be made by substituting appropriate values into eqns. 2–4. For $m = 6$, $\tau_a = 0.1 f_0^{-1}$ and $Q = 1.6$, with the modelled bias current and voltage modulation, $\Delta f_0 / I_{so} = 8.8$ MHz μA^{-1}. This slope is plotted as a solid line in Fig. 3. The modelled values for electron and hole tuning lie above and below this line, respectively. This is because the analytic theory assumes equal avalanche ionisation coefficients for electrons and holes, whereas in silicon those for electrons are much greater than those for holes. Thus electron injection produces a much greater tuning effect than hole injection. With this restriction, agreement between the analytic theory and the modelling results is seen to be good.

4 Experimental work

The devices used were single-drift silicon impatts mounted in quartz ring packages as shown in Fig. 4. All measurements were carried out using the well known resonant cap circuit design [8] shown in Fig. 5A. At a current of 120 mA, the output power obtained was 55 mW and the efficiency was 3.1%, which is in good agreement with the computer model result of 3.6%, bearing in mind that the computer model neglects circuit losses.

A GaAs/GaAlAs laser emitting at 850 nm was used as the light source for the optical tuning experiments.

The laser was supplied with an optical fibre output of 50 125 μm graded index fibre which was coupled to the edge of the active device through a small hole in the oscillator cavity wall. The fibre was brought into very close proximity with the quartz ring of the diode package, and its position was then optimised for maximum tuning effect using a micromanipulator. Fig. 5B gives details of the configuration used. The laser package also contained a
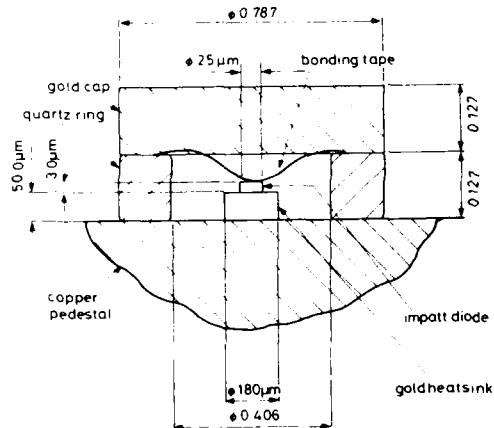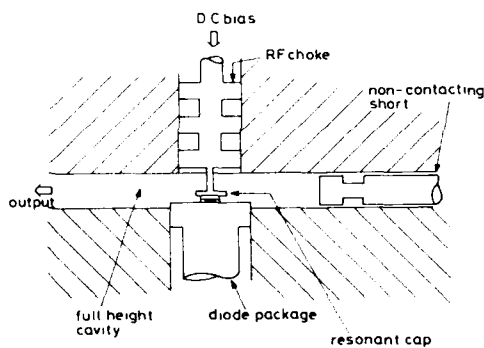

Fig. 4 *Impatt diode in quartz ring package*
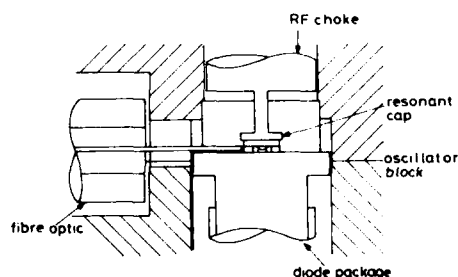

Fig. 5A *Impatt oscillator cavity*

Fig. 5B *Coupling of optical fibre to Impatt diode*
Vertical section through centre of diode

monitor photodiode which was used, after calibration, to determine the laser output power.

Using this arrangement, optically generated reverse saturation currents of up to 20.5 μA were obtained for an optical power, measured at the fibre end, of 3 mW. From eqn. 5 this power should be sufficient to generate a current

of about 1.9 mA for a quantum efficiency of 0.9. The low measured coupling efficiency of 1.1% is due partly to refraction in the quartz ring package and partly to the very small height of the impatt structure, around 3 μm, compared with the fibre core diameter of 50 μm.

Fig. 6. shows a typical spectrum analyser display for an

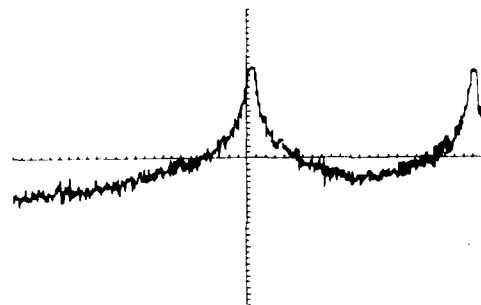**Fig. 6** *Optical tuning of 9.40 MHz at a centre frequency of 91.826 GHz*
Frequency span 20 MHz, optically generated current 20.3 μA

oscillator undergoing optical tuning. In this example the bias current was 100 mA, giving a free-running frequency of 91.83 GHz, which is represented by the peak at the centre of the display. The right-hand peak is the output of the oscillator with an optically generated current of 20.3 μA. The frequency shift obtained was 9.4 MHz.

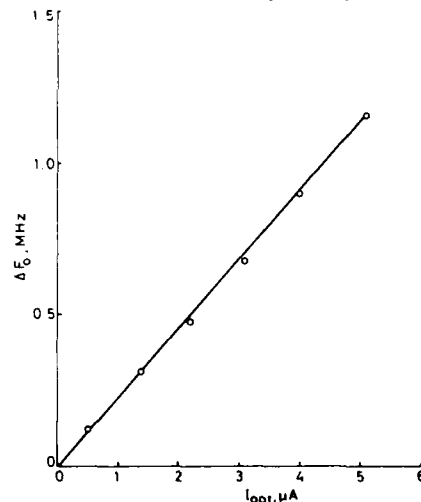Fig. 7 is a plot of oscillation shift against optically generated current for another impatt sample at a bias current

Fig. 7 *Frequency tuning against optically generated current*

of 120 mA. The shift is proportional to current as predicted by eqn. 2. In order to compare the tuning slope with theory it is necessary to know the Q-factor of the oscillator. This was measured by injection locking [9]. From measurements of the injected power, the impatt oscillator output power and the locking range the Q was determined from

$$Q = \frac{2\omega_0}{2\Delta\omega_e} \sqrt{\frac{P_i}{P_o}} \tag{6}$$

where ω_0 is the free running impatt frequency, $2\Delta\omega_e$ is the total locking range, P_i is the injected power and P_o is the

impatt output power. Measurements on the oscillator of Fig. 7 gave a Q of about 200. From the tuning character-istic, Fig. 7, $d(\Delta f)/dI_w = 225$ KHz.μA^{-1}. $F_a\{x\}$ was esti-mated from the measured output power to be 27, giving a calculated tuning slope of 253 KHz.μA^{-1} from eqn. 2. There is thus good agreement between predicted and mea-sured results, particularly when bearing in mind that the theory assumes equal ionisation coefficients for holes and electrons.

5   Discussion

Optical tuning has been demonstrated for a W-Band impatt oscillator. The maximum frequency shift obtained was 9.4 MHz using a 3 mW semiconductor laser. This figure is very small and can be explained by the very low coupling efficiency (1.1%) of light from the laser output to the impatt device due to the illumination geometry used. If this coupling efficiency could be increased to 65%, which is a typical value for high speed photodiodes, the tuning range should increase to over 600 MHz, which would be useful in many systems applications.

Methods of improving coupling include the replacement of the quartz ring package with one using quartz standoffs and the use of lenses or mirrors to concentrate the incident light. A more promising approach, however, is to illumi-nate the top or bottom surface of the device rather than the edge, as has already been demonstrated at lower fre-quencies by Vyas et al. [10] and Chiu and Freyer [11]. This involves the fabrication of special millimetre-wave impatt structures and forms the basis of continuing work on this project.

Experimental results showed a linear relationship between frequency shift and optically injected current in agreement with the analytical and computer models devel-oped during this study. Measured tuning slopes were also in good agreement with those predicted theoretically, although the tuning slope of the oscillator used in the com-puter modelling studies was much larger than that for the experimental oscillator, since a Q of 1.5 was used com-pared with a Q of around 200 for the practical oscillator.

The simple analytical theory has been shown to give good agreement with a large-signal time-domain computer model. The computer model has shown that electron injec-tion gives a considerably greater tuning effect than hole injection, which is an important consideration when struc-tures are to be fabricated to enable the top or bottom device surfaces to be illuminated.

An initial investigation of the tuning-speed modelling has shown that very fast tuning is possible, which is obvi-ously a key factor in systems applicability. It is expected that the oscillator Q would be the fundamental limitation in this regard.

The main area for development of the computer model is the improvement of the oscillator circuit from the very simple one of Fig. 1 to one which would model the actual configuration used, Fig. 5A.

Optical tuning provides a technique for controlling the frequency of impatt oscillators which offers electrical iso-lation and ease of control signal distribution through optical fibres. With further development this technique will prove to be attractive for a number of millimetre-wave radar and communication system applications

7   References

1 KIEHL, R.A., and EERNISSE, F.P. 'Control of TRAPATT oscil-lations by optically generated carriers', IEEE Trans., 1977, ED-24, pp. 275-277
2 YEN, H.W., and BARNOSKI, M.K. 'Optical injection locking and switching of transistor oscillators', Appl. Phys. Lett., 1978, 32, pp. 182-184
3 SALLES, A.A. 'Optical control of GaAs MESFETs', IEEE Trans., 1983, MTT-31, pp. 812-820
4 VYAS, H.P., GUTMANN, R.J., and BORREGO, J.M. 'Optical-microwave effects in IMPATT diode oscillators', IEEE MTT Symp Tech. Digest, 1979, pp. 188-190
5 FORREST, J.R., and SEEDS, A.J. 'Analysis of the optically con-trolled IMPATT (OPCAD) oscillator', IEE J. Solid-State & Electron Dev., 1979, 3, pp. 161-169
6 READ, W.T. 'A proposed high-frequency negative-resistance diode', Bell Syst. Tech. J., 1958, 37, pp. 401-446
7 BLAKEY, P.A., GIBLIN, R.A., and SEEDS, A.J. 'Large-signal time-domain modelling of avalanche diodes', IEEE Trans., 1979, ED-26, pp. 1718-1728
8 MISAWA, T., and KENYON, N.D. 'An oscillator circuit with cap structure for millimetre-wave IMPATT diodes', IEEE Trans., 1970, MTT-18, pp. 969-970.
9 ADLER, R. 'A study of locking phenomena in oscillators', Proc. IRE, June 1946, pp. 351-357
10 VYAS, H.P., GUTMANN, R.J., and BORREGO, J.M. 'Hole and electron photo-current effects on Impatt oscillators', IEE Proc. I, Solid-State & Electron Dev., 1980, 127, pp. 126-132
11 CHIU, C., and FREYER, J. 'Frequency modulation of Impatt diodes by optical illumination', ibid., 1984, 31, pp. 28-30

APPENDIX D

403

The Optical Control of IMPATT Oscillators

A. J. SEEDS, J. F. SINGLETON, S. P. BRUNT, AND J. R. FORREST

Abstract—This paper describes methods of controlling the frequency of IMPATT oscillators using optical rather than electrical signals. Analytic theories of optical tuning and injection locking are presented. Results from a comprehensive large signal computer model of the optically controlled IMPATT oscillator are given, illustrating the importance of the composition of the optically generated current on the optical control performance and demonstrating the capability of optical control for rapid frequency tuning. Finally, recent experimental work on optical tuning effects in W-Band IMPATT oscillators is presented.

I. INTRODUCTION

THE EASE of transmission of high rate intensity modulated optical signals through single mode optical fibres suggests their use for signal distribution in complex microwave systems such as phased-array radars [1], [2]. For active phased arrays, where each element has its own microwave power source, considerable simplification results from direct optical control of the active device.

Three distinct modes of control can be identified. In the first the optical signal alters the negative resistance properties of the active device so as to drive it into or out of oscillation: this is known as optical switching. The second mode uses an optical signal of lower intensity to induce optical tuning of the oscillator frequency. Finally, illumination with an optical signal, intensity modulated at a frequency close to the free-running oscillator frequency, one of its harmonics or subharmonics, can produce optical injection locking.

Optical control of a variety of microwave devices has been demonstrated. Yen and Barnoski [3] have investigated optical switching and subharmonic injection locking in bipolar transistor oscillators. Optical tuning of the oscillation frequency in MESFET oscillators has been demonstrated by Sun *et al.* [4] as has optical injection locking by Salles and Forrest [5]. Turning to two terminal devices, optical tuning and switching of TRAPATT oscillators operating at frequencies up to 1.5 GHz has been reported by Kiehl [6].

At the higher microwave frequencies the IMPATT diode oscillator is one of the most powerful solid-state

sources [7]. However, the power and impedance levels involved make tuning by conventional means, such as YIG spheres or varactor diodes, extremely difficult. This has led to considerable work on the optical control of IMPATT diodes, in which optical switching [8], [9], tuning [10], [11] and injection locking [12], [13] have all been demonstrated. In addition, optical carrier injection can assist in stabilizing the level of reverse saturation current in the device, leading to an improvement in oscillator noise [14], [15].

The object of this paper is to present analytical and computer modelling studies of optical tuning and injection locking in IMPATT oscillators, together with recent experimental measurements of optical tuning in W-Band IMPATT oscillators.

II. ANALYTIC THEORY OF OPTICAL CONTROL

A. IMPATT Diode Model

Illumination of an IMPATT diode with light having a photon energy greater than the band gap of the semiconductor material from which it is fabricated results in the generation of electron-hole pairs within the device. These carriers alter the timing of the avalanche cycle, thus producing a change in oscillation frequency. If the intensity of the incident optical signal is modulated a varying current is generated in the diode which, following avalanche multiplication, can be used to injection lock the IMPATT oscillator.

A general analysis of the optically controlled IMPATT oscillator is made difficult by the extreme nonlinearity of the avalanche multiplication process. However, if it is assumed that all carrier motion is at saturated velocity v_s, and that electrons and holes have equal ionization coefficients α, a simple expression for the avalanche current density J can be written [16]:

$$\frac{\tau_a}{2}\frac{dJ}{dt} = J\left[\int_0^{L_a} \alpha dz - 1\right] + J_s \tag{1}$$

where L_a is the avalanche zone length, τ_a ($= L_a/v_s$) is the avalanche zone transit time and J_s is the total reverse saturation current density including both optically and thermally generated components:

$$J_s = J_{s0} + J_{s1} \sin(\omega t + \phi). \tag{2}$$

Here J_{s0} is the constant thermally and optically generated saturation current and J_{s1} is the peak value of an optically generated locking current of frequency ω and arbitrary phase constant ϕ.

To solve (1), an expression for the electric field dependence of the ionization coefficient α is required. A useful model is

$$\alpha = \alpha_0 \left(\frac{E}{E_0} \right)^m \qquad (3)$$

where E is the electric field, m is an ionization nonlinearity constant ($m \approx 6$ for silicon) and α_0 and E_0 are constants. Assuming that the avalanche zone is uniformly doped, that the field in the drift zone is much less than the peak field within the diode and that the voltage swing across the diode is moderate, then, following Carroll [17], the ionization integral in (1) can be evaluated to give

$$\frac{dJ}{dt} = \frac{2(m+1)}{\tau_a} J \left[\frac{m}{4} \left(\frac{E_1}{E_{p0}} \right)^2 - \frac{E_b}{E_{p0}} \right.$$

$$\left. + \frac{E_1}{E_{p0}} \sin(\omega t + \delta) \right] + \frac{2J_s}{\tau_a} \qquad (4)$$

where harmonic terms are neglected and the peak electric field E_p is represented by

$$E_p = E_{p0} - E_b + E_1 \sin(\omega t + \delta) \qquad (5)$$

for a diode terminal voltage

$$v = V_{p0} + L(E_1 \sin(\omega t) - E_b). \qquad (6)$$

Here E_b is a back bias field resulting from the combined effects of ionization nonlinearity, reverse saturation current and carrier space charge λ, E_1 is the peak value of the modulated component of electric field, L is the total depletion width, and V_{p0} the breakdown voltage. Equation (6) assumes the diode to be embedded in an oscillator circuit of moderately high Q factor, so that the voltage variation will be nearly sinusoidal, and that the diode remains punched-through over the whole RF cycle. It is also assumed that the oscillator is locked to the incident modulated optical signal, where present, to give an oscillation frequency of ω. The injection locking range can then be found from the limiting conditions on the phase angle ϕ. The phase angle δ is used to represent back bias and carrier space charge effects; details of its evaluation are given by Cullen and Forrest [18].

Equation (4) is a linear, first order equation, and can be solved using an integrating factor expanded in terms of modified Bessel functions. Following integration across the drift zone the fundamental component of the device external conduction current can be written

where τ_d is the drift zone transit time and $I_n\{X\}$ are modified Bessel function coefficients of order n and argument

$$X = \frac{2(m+1)E_1}{\omega \tau_a E_{p0}}. \qquad (8)$$

In deriving (7) it has been assumed that $J_{s1} \ll J_{s0} \ll J_{dc}$ so that the effect of the optically injected current on the diode bias voltage is small.

Equation (7) contains three clearly identifiable terms; the term in $\cos(\omega t + \delta)$ represents the fundamental component of the main avalanche current, that in $\sin(\omega t + \delta)$ a quadrature term that alters the phasing of the avalanche current in response to reverse saturation current J_{s0}, while the term in $\cos(\omega t + \phi)$ represents the optical injection locking signal. The first two terms can be combined by introducing a modified phase angle δ_s:

$$\delta_s = \delta + \sin^{-1} \left(2 \frac{J_{s0}}{J_{dc}\omega\tau_a} F_a\{X\} \right) \qquad (9)$$

where the avalanche gain factor for optical tuning $F_a\{X\}$ is defined by

$$F_a\{X\} = I_0^2\{X\} + \frac{I_0\{X\}}{I_1\{X\}}$$

$$\cdot \lambda \sum_{n=1}^{\infty} \frac{(-1)^n (2n+1) I_{n+1}\{X\} I_n\{X\}}{n(n+1)}. \qquad (10)$$

Equation (7) can then be rewritten

$$J_1 = -2J_{dc} \frac{\sin\left(\frac{\omega\tau_d}{2}\right)}{\left(\frac{\omega\tau_d}{2}\right)} \frac{I_1\{X\}}{I_0\{X\}} \cos\left(\omega\left(t - \frac{\tau_d}{2}\right) + \delta_s\right)$$

$$- \frac{2J_{s1}}{\omega\tau_a} \frac{\sin\left(\frac{\omega\tau_d}{2}\right)}{\left(\frac{\omega\tau_d}{2}\right)} F_b\{X\} \cos\left(\omega\left(t - \frac{\tau_d}{2}\right) + \phi\right) \qquad (11)$$

where $F_b\{X\}$ is an avalanche gain factor for optical injection locking:

$$J_1 = \frac{\sin\left(\frac{\omega\tau_d}{2}\right)}{\left(\frac{\omega\tau_d}{2}\right)} \left[\begin{array}{l} -2J_{dc} \dfrac{I_1\{X\}}{I_0\{X\}} \cos\left(\omega\left(t - \frac{\tau_d}{2}\right) + \delta\right) \\[2ex] +4J_{s0} \left[\dfrac{I_0\{X\} I_1\{X\}}{\omega\tau_a} + \sum_{n=1}^{\infty} \dfrac{(-1)^n (2n+1) I_{n+1}\{X\} I_n\{X\}}{n(n+1)\omega\tau_a} \right] \cdot \sin\left(\omega\left(t - \frac{\tau_d}{2}\right) + \delta\right) \\[2ex] -J_{s1} \left[\dfrac{2I_0^2\{X\} - I_1^2\{X\} - I_1\{X\} I_3\{X\}}{\omega\tau_a} - 4\sum_{n=2}^{\infty} \dfrac{(-1)^n I_n^2\{X\}}{(n-1)(n+1)\omega\tau_a} \right] \cdot \cos\left(\omega\left(t - \frac{\tau_d}{2}\right) + \phi\right) \end{array} \right] \qquad (7)$$

$$F_b\{X\} = I_0^2\{X\} - \frac{I_1^2\{X\} + I_1\{X\} I_3\{X\}}{2}$$

$$- 2 \sum_{n=2}^{\infty} \frac{(-1)^n I_n^2\{X\}}{(n-1)(n+1)}. \tag{12}$$

Equations (9)–(12) represent a generalization of an earlier analysis [19] and enable predictions of optical tuning and injection locking performance to be made when coupled with a suitable oscillator circuit model.

The avalanche gain factors defined by (10) and (12) are strong functions of the peak RF voltage swing across the IMPATT diode through the Bessel function argument dependence on peak modulated electric field. equation (8). In evaluating these gain factors the number of terms in the Bessel function series that need to be taken into account depends on the argument value X. A typical IMPATT might have

$$\tau_a = 0.2\tau_d = 0.2\pi/\omega_0 \tag{13}$$

where ω_0 is the free running oscillator frequency. Thus, for $\omega \approx \omega_0$, $m = 6$ and a maximum voltage modulation of 25 percent, $X \le 5.6$. Fig. 1 shows the variation in $F_a\{X\}$ and $F_b\{X\}$ with X for $n \le 1$ to 4. It can be seen that truncating the series at $n = 3$ provides sufficient accuracy for most purposes.

For $X = 4.5$, corresponding to about 20-percent voltage modulation $F_a\{X\} = 78$ and $F_b\{X\} = 209$ showing that avalanche gain enhances the optical control sensitivity considerably.

B. Oscillator Circuit Model

To obtain predictions of the optical tuning and locking ranges a circuit model for the oscillator is required. Fig. 2 shows a simple lumped model in which the IMPATT is represented by an admittance Y_1 ($= G_1 + jB_1$) and the load by a parallel LR circuit of admittance Y_L ($= G_L + jB_L$). The optical injection locking signal is represented by a current generator i_l defined from equation (11) as

$$i_l = -\frac{2J_{s1}AF_b\{X\}}{\omega\tau_a} \frac{\sin\left(\frac{\omega\tau_d}{2}\right)}{\left(\frac{\omega\tau_d}{2}\right)}$$

$$\cdot \exp j\left(\omega\left(t - \frac{\tau_d}{2}\right) + \phi\right) \tag{14}$$

where A is the diode area. From (6) the RF voltage across the diode is given by
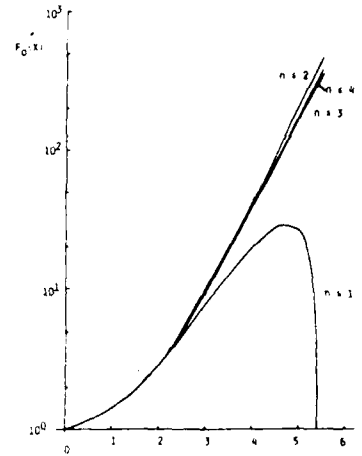
$$v_1 = -jV_1 \exp j(\omega t) \tag{15}$$

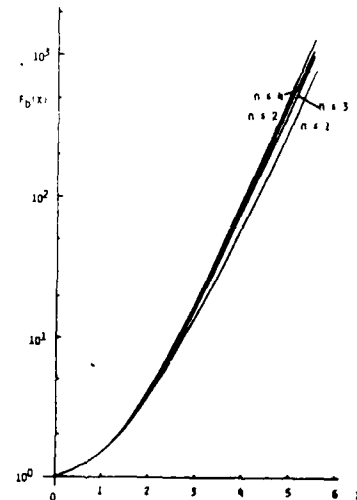where $V_1 = E_1 L$. Thus the circuit equation for Fig. 2 is

$$i_l = (Y_1 + Y_L) v_1 \tag{16}$$

C. Optical Tuning Predictions

If there is no injected locking signal G_L and B_L are obtained from (11), (15), and (16), setting $J_{s1} = 0$ and add-

Fig 1 Variation of avalanche gain factors for optical control with parameter X. (a) $F_a\{X\}$. (b) $F_b\{X\}$.
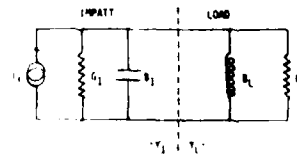

Fig 2 Equivalent circuit for optically controlled IMPATT oscillator

ing the diode depletion susceptance ωC_d to the active susceptance:

$$G_L = \frac{4I_{dc}\sin\left(\frac{\omega\tau_d}{2}\right)I_1\{X\}}{V_1\omega\tau_d I_0\{X\}}\sin\left(\frac{\omega\tau_d}{2} - \delta_s\right) \qquad (17)$$

$$B_L = \frac{4I_{dc}\sin\left(\frac{\omega\tau_d}{2}\right)I_1\{X\}}{V_1\omega\tau_d I_0\{X\}}\cos\left(\frac{\omega\tau_d}{2} - \delta_s\right) - \omega C_d \qquad (18)$$

where $I_{dc} = J_{dc}A$. Dividing (18) by (17) and defining B_L as $B_L = -1/(\omega L_L)$ gives

$$\omega C_d - \frac{1}{\omega L_L} = G_L\cot\left(\frac{\omega\tau_d}{2} - \delta_s\right). \qquad (19)$$

The tuning sensitivity can be obtained by assuming that $\omega = \omega_0 + \Delta\omega$, where $\omega_0 = (L_L C_d)^{-0.5}$. Then for $\delta_s \ll \pi/2$ substitution of (9) in (19) with assumption (13) yields

$$\Delta\omega \approx \frac{G_L}{2C_d}\left[\delta + 2\frac{I_{s0}F_a\{X\}}{I_{dc}\omega_0\tau_a}\right] \qquad (20)$$

where $I_{s0} = J_{s0}A$. The optical frequency tuning slope is then

$$\frac{d(\Delta\omega)}{dI_{s0}} = \frac{G_L F_a\{X\}}{C_d I_{dc}\omega_0\tau_a}. \qquad (21)$$

Defining oscillator Q factor as

$$Q = \frac{\omega_0 C_d}{G_L} \qquad (22)$$

(21) can be rewritten

$$\frac{d(\Delta\omega)}{dI_{s0}} = \frac{F_a\{X\}}{QI_{dc}\tau_a}. \qquad (23)$$

This shows that the optical tuning slope is proportional to the avalanche gain factor $F_a\{X\}$ and inversely proportional to the oscillator Q.

D. *Optical Injection Locking Predictions*

In optical injection locking, $i_l \neq 0$. Substituting (14), (15), (17), and (18) in (16), with the assumption (13) and for $\delta_s \ll \pi/2$, gives the real part of (16) as

$$\frac{4I_{s1}F_b\{X\}}{\pi\omega_0\tau_a V_1}\sin\phi = \omega C_d - \frac{1}{\omega L_L} \qquad (24)$$

where $I_{s1} = J_{s1}A$.

Applying the Adler [20] condition, $\sin\phi = \pm 1$, the locking range is found to be

$$2\Delta\omega_L = \frac{4I_{s1}F_b\{X\}}{\pi\omega_0\tau_a V_1 C_d}. \qquad (25)$$

This can be restated in a form similar to the Adler locking equation by substituting from (22) with (17) and assumption (13):

$$2\Delta\omega_L = 5F_b\{X\}\frac{I_0\{X\}\omega_0 I_{s1}}{I_1\{X\}QI_{dc}}. \qquad (26)$$

Thus the locking range is proportional to the optically injected current I_{s1} and the avalanche gain factor $F_b\{X\}$, and inversely proportional to the oscillator Q.

III. COMPUTER MODELING STUDIES

The analytic theory presented in the previous section requires a number of approximations to produce tractable results. Of particular importance is the assumption of equal ionization coefficients for electrons and holes. In silicon the coefficient for electrons is an order of magnitude higher than that for holes, over a wide range of electric field. The optical tuning behavior is thus considerably dependent on the composition of the optically generated current entering the avalanche zone, and hence on the illumination configuration [21].

To investigate these effect a large signal time-domain computer model for the optically controlled IMPATT has been developed. This is based on the numerical methods described by Blakey et al. [22], while the modifications required to model optical carrier generation effects have been detailed elsewhere [23]. The model uses an explicit solution in one spatial dimension and time, with the active region of the diode divided into, typically, 100 mesh-points. Output from the model is in terms of terminal current and voltage as a function of time.

A. *Large Signal Admittance Studies*

By coupling the diode to an RF voltage source plots of large signal admittance against frequency and peak RF voltage can be obtained. Fig. 3 shows typical results for an X-Band p^+-n-n^+ silicon device, at a bias current of 600-A cm^{-2}. Carrier generation in the p^+ and n^+ regions has been neglected so that the optically generated charge comprises electron-hole pairs generated in the n region. An exponential optical absorption profile is assumed, with an absorption coefficient of 6×10^5 m^{-1}, a value representative of a He-Ne LASER illuminating silicon at a temperature of 500 K. In Fig. 3(a) the diode is unilluminated. The device conductance is seen to be negative and decreasing in magnitude with increased voltage swing, as predicted by analytic theory, equations (16) and (17).

In Fig. 3(b) the diode has been illuminated from the n^+ region so that the majority of the optically generated carriers entering the avalanche zone are holes. The magnitude of the device conductance is reduced, and this reduction is more pronounced at the higher voltage swings, in accordance with (9) and (17). Indeed, for a peak RF voltage of 40 V, oscillatory solutions are no longer possible; this is the basis of the optical switching effect [6], [8], [9].

In Fig. 3(c) the direction of the illumination has been reversed, so that the majority of the optically generated carriers entering the avalanche zone are electrons. This results in a much greater admittance change than that for
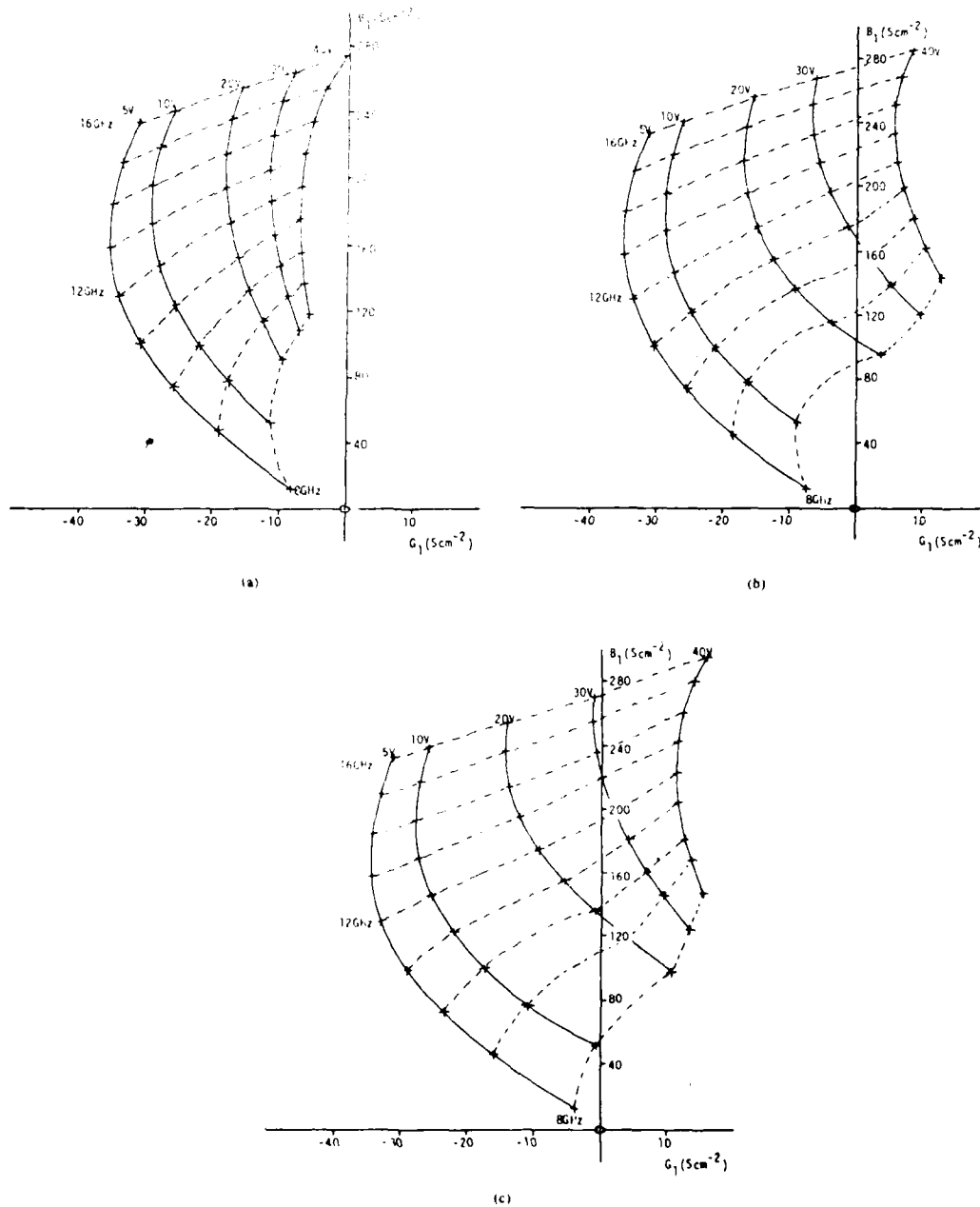
(a)

(b)

(c)

Fig 3 Effect of illumination on large signal admittance of p^+-n-n^+ X-Band silicon IMPATT diode (a) Unilluminated diode (b) Diode illuminated from n^+ region Optically injected current density 3 A cm^{-2} (c) Diode illuminated from p^+ region Optically injected current density 1 A cm^{-2}
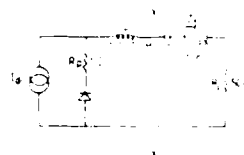
Fig. 4. W-Band IMPATT oscillator equivalent circuit used in computer modeling studies.

n$^+$ illumination due to the higher ionization coefficient for electrons in silicon. Thus superior optical control performance would be anticipated from this illumination configuration.

B. Optical Tuning Studies

In order to obtain a direct comparison with the optical tuning theory of Section II-C the IMPATT diode model was coupled to the simple oscillator circuit model shown in Fig. 4. L_p represents the diode bond wire inductance, R_p the diode parasitic resistance, R_L the load resistance, C the dc block capacitance and Z_t a quarter-wave transformer. If L_p is chosen to resonate with the capacitive susceptance of the diode the impedance seen looking towards the diode at plane $X - X'$ is real and negative. The amplitude of the oscillation is then determined by selecting Z_t to match R_L to the impedance at $X - X'$ for the required operating point. For comparison with the experimental work of Section IV the diode modeled in this part of the study was a W-Band p$^+$-n-n$^+$ silicon device, with oscillator circuit values chosen to give an oscillation frequency of 94 GHz.

To illustrate the maximum variation in tuning slope with optically generated current composition two extreme illumination configurations were used. In the first, electrons were injected into the depletion zone from the p$^+$ region whereas in the second holes were injected from the n$^+$ region. Fig. 5 shows the optical tuning characteristics obtained from optically generated current densities of up to 2 A · cm^{-2}, with a bias current density of 28.45 kA · cm^{-2}. The change in frequency with injected current is linear, as expected from (20), and the tuning slope for electron injection is some 4.5 times that for hole injection. Also shown in Fig. 5 is the slope calculated from (23). This lies between the two modeled curves owing to the assumption of equal ionization coefficients in the analytic theory.

C. Transient Study

One of the attractions of optical tuning is that fast tuning should be possible owing to the elimination of varactor charging time and similar delays. Since the computer model operates in the time-domain transient studies are readily carried out. Fig. 6 shows the tuning transient resulting from a step change in optically injected electron current from 0–2 A · cm^{-2} in the W-Band oscillator modeled previously. Ninety percent of the frequency change
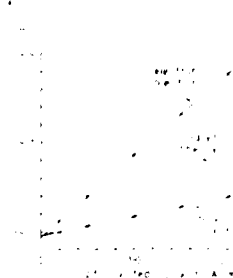

Fig. 5. Comparison between computer model and analytic theory for optical tuning characteristics of W-Band oscillator.
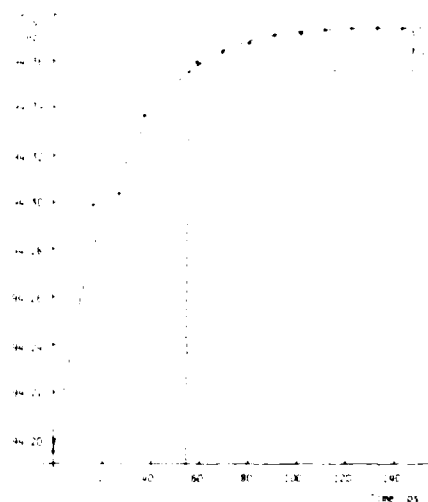

Fig. 6. Modeled optical tuning transient for W-Band IMPATT oscillator. $J_d = 28.45$ kA · cm^{-2}, $J_o = 0 \rightarrow 2$ A · cm^{-2}.

was achieved in 55 ps, which compares favorably with conventional techniques. This may afford novel systems possibilities, subject to the fundamental limitation on tuning speed due to the oscillator Q factor.

IV. EXPERIMENTAL WORK

Previous work on the optical control of IMPATT oscillators has mostly been carried out at frequencies below 18 GHz [8]–[13]. The object of this section is to describe recent experimental work on the optical tuning of W-Band (≈94 GHz) IMPATT oscillators.

The diodes used in this work were silicon single-drift p$^+$-n-n$^+$ structures fabricated at GEC Hirst Research Laboratories. These were mounted in quartz ring packages and used in resonant cap type oscillator circuits, having external Q factors of about 200.

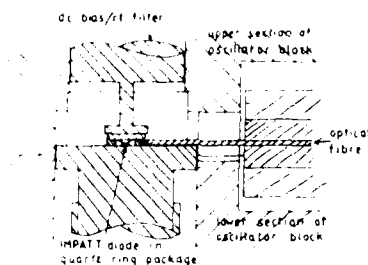The optical control signal was generated by a GaAs/GaAlAs laser emitting at a wavelength of 850 nm.

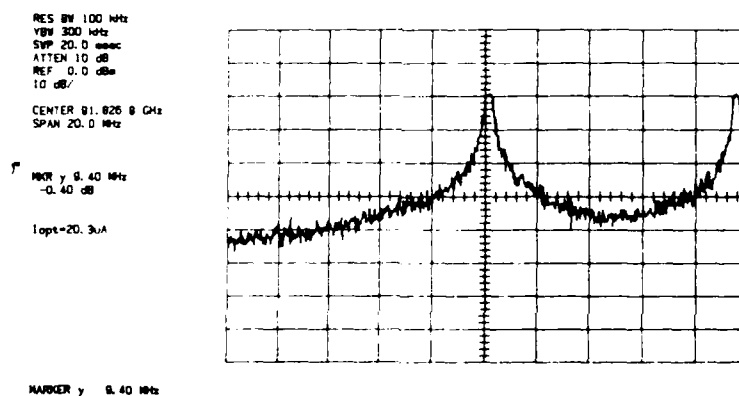Fig. 7 Experimental optically controlled W-Band IMPATT oscillator

Fig. 8 Spectrum analyzer display for W-Band IMPATT oscillator showing optical tuning

A 50/125-μm graded index optical fiber was used to couple the output to the edge of the IMPATT diode, as shown in Fig. 7. The position of the fiber was adjusted to give maximum optically generated current using a micromanipulator. With this arrangement optically generated reverse saturation currents of up to 20.5 μA were obtained for an optical power of 3 mW. The optically generated current can be related to the optical power by

$$I_{s0} = C\,\frac{\eta_q e\lambda P_{op}}{hc} \qquad (27)$$

where P_{op} is the optical power, η_q the internal quantum efficiency, λ the optical wavelength, e the electronic charge, c the velocity of light in vacuo, and C a dimensionless coupling efficiency. Assuming $\eta_q \approx 1$ at the operating wavelength gives $C = 1$ percent. This low value is due partly to refraction in the quartz ring package and partly to the small height of the IMPATT structure, around 3 μm, compared with the fiber core diameter of 50 μm.

Fig. 8 shows a typical spectrum analyzer display for an oscillator bias current of 100 mA, giving a free-running frequency of 91.83 GHz. The center peak is the output of the unilluminated oscillator, while the right-hand peak is

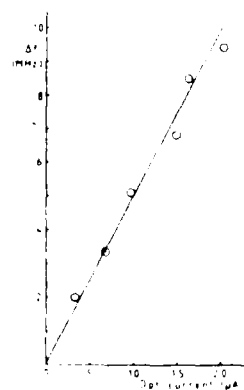

Fig. 9 Measured optical tuning characteristic for W-Band IMPATT oscillator

the output of the oscillator with an optically generated current of 20.3 μA, giving a frequency shift of 9.4 MHz.

Fig. 9 is a plot of oscillation frequency against optically generated current. The shift in frequency is proportional to injected current as would be expected from (20) with

small injected current. The tuning slope can be compared with analytic theory [23], having estimated the avalanche gain factor $F_a(X)$ from the measured output power [19]. For $\tau_a = 0.7$ ps and $Q = 200$ the predicted tuning slope is 550 kHz $\cdot$ μA^{-1}. From Fig. 9 the measured value is 490 kHz $\cdot$ μA^{-1}. There is thus good agreement, particularly bearing in mind the equal ionization coefficients approximation inherent in the theory. These tuning slopes are considerably less than those in the computer modeling work of Section III-B because of the low Q oscillator circuit modeled, Fig. 4.

V. CONCLUSION

An analytic theory for the optical control of IMPATT diodes has been described. This theory has been supplemented by results from large signal computer modeling studies. Recent experimental measurements on optical tuning in W-Band IMPATT oscillators have been presented, showing good agreement with the theoretical work.

The computer modeling studies have shown the limitations of the equal ionization coefficients assumption used in the analytic theory. However, the theory remains useful in identifying the effect of device and circuit parameters on optical control performance. The analytic theory assumes that the optically generated circuit is sufficiently small not to alter the diode bias voltage or oscillation amplitude significantly. Chiu and Freyer [11] have shown that where this condition is not met significant increases in optical tuning sensitivity arise from thermal effects.

The computer modeling study has indicated that optical tuning is capable of rapid frequency scanning, a feature of considerable systems interest. Experimental work is currently under way to test this prediction.

Optical tuning of a W-Band IMPATT oscillator has been demonstrated over a range of 10 MHz. The main cause of this limited tuning range is the poor coupling efficiency between the optical source and the IMPATT diode. An important area for further work is the fabrication of special millimeter-wave IMPATT structures, having an improved optical response, such as have already been developed at lower frequencies [21]. If the coupling efficiency could be increased to 65 percent, a typical value for high speed photodiodes, the tuning range would increase to over 600 MHz in the oscillator described.

Optical injection locking, as described in Section II-D, has been demonstrated at microwave frequencies using directly modulated semiconductor lasers as optical sources [12], [13]. However the maximum modulation frequency is limited by carrier and photon lifetime considerations. Laser heterodyning [24] offers a technique for extending optical injection locking into the millimeter-wave frequency range if the formidable technological difficulties can be overcome.

It is hoped that the work described has illustrated the potential of optical control. Although much further work

remains to be done, the attractiveness of optical signal processing and distribution should ensure a place for such techniques in future microwave and millimeter-wave systems.

REFERENCES

[1] J. R. Forrest, F. P. Richards, and A. A. Salles, "Optical fibre networks for signal distribution and control in phased array radars," in *Proc. Int. Conf. Radar '82* (London, England), 1982, pp. 408–412.

[2] P. G. Sheehan and J. R. Forrest, "The use of optical techniques for beam forming in phased arrays," *Proc. SPIE*, vol. 477, pp. 82–89.

[3] H. W. Yen and M. K. Barnoski, "Optical injection locking and switching of transistor oscillators," *Appl. Phys. Lett.*, vol. 32, pp. 182–184, 1978.

[4] H. J. Sun, R. J. Gutman, and J. M. Borrego, "DC and pulse-light illuminated optical responses of microwave GaAs-MESFET oscillators," *Proc. Inst. Elec. Eng.*, vol. 131 I, pp. 31–37, 1984.

[5] A. A. Salles and J. R. Forrest, "Initial observations of optical injection locking of GaAs metal semiconductor field effect transistor oscillators," *Appl. Phys. Lett.*, vol. 38, pp. 392–394, 1981.

[6] R. A. Kiehl, "Behavior and dynamics of optically controlled TRAPATT oscillators," *IEEE Trans. Electron. Devices*, vol. ED-25, pp. 703–710, 1978.

[7] S. M. Sze, *Physics of Semiconductor Devices.* New York: Wiley, 1981, p. 612.

[8] H. W. Yen, M. K. Barnoski, R. G. Hunsperger, and R. T. Melville, "Switching of GaAs IMPATT diode oscillator by optical illumination," *Appl. Phys. Lett.*, vol. 31, pp. 120–122, 1977.

[9] R. A. Kiehl, "Optically induced AM and FM in IMPATT diode oscillators," *IEEE Trans. Electron Devices*, vol. ED-27, pp. 426–432, 1980.

[10] H. P. Vyas, R. J. Gutmann, and J. M. Borrego, "Leakage current enhancement in IMPATT oscillators by photoexcitation," *Electron. Lett.*, vol. 13, pp. 189–190, 1977.

[11] C. Chiu and J. Freyer, "Frequency modulation of IMPATT diodes by optical illumination," *Proc. Inst. Elec. Eng.*, vol. 131, pp. 28–30, 1984.

[12] A. J. Seeds and J. R. Forrest, "Initial observations of optical injection locking of an X-Band IMPATT oscillator," *Electron. Lett.*, vol. 14, pp. 829–830, 1978.

[13] H. W. Yen, "Optical injection locking of Si IMPATT oscillators," *Appl. Phys. Lett.*, vol. 36, pp. 680–683, 1980.

[14] A. J. Seeds and J. R. Forrest, "Reduction of FM noise in IMPATT oscillators by optical illumination," *Electron. Lett.*, vol. 17, pp. 865–866, 1981.

[15] P. M. Pitner, R. J. Gutmann, and J. M. Borrego, "Photocurrent effects on noise in silicon IMPATT oscillators," *Proc. Inst. Elec. Eng.*, vol. 128 I, pp. 149–152, 1982.

[16] W. T. Read, "A proposed high-frequency negative resistance diode," *Bell Syst. Tech. J.*, vol. 37, pp. 401–446, 1958.

[17] J. E. Carroll, *Hot Electron Microwave Generators.* London: Arnold, 1970, pp. 197–212.

[18] A. L. Cullen and J. R. Forrest, "Analytic theory of the IMPATT diode and its application to calculations of oscillator locking characteristics," *Proc. Inst. Elec. Eng.*, vol. 121, pp. 1467–1474, 1974.

[19] J. R. Forrest and A. J. Seeds, "Analysis of the optically controlled IMPATT (OPCAD) oscillator," *IEE J. Solid-State and Electron Devices*, vol. 3, pp. 161–169, 1979.

[20] R. Adler, "A study of locking phenomena in oscillators," *Proc. IRE*, 1946, 34, pp. 351–357.

[21] H. P. Vyas, R. J. Gutmann, and J. M. Borrego, "Hole and electron photocurrent effects on IMPATT oscillators," *Proc. Inst. Elec. Eng.*, vol. 127 I, pp. 126–132, 1980.

[22] P. A. Blakey, R. A. Giblin, and A. J. Seeds, "Large signal time-domain modelling of avalanche diodes," *IEEE Trans. Electron Devices*, vol. ED-26, pp. 1718–1728, 1979.

[23] A. J. Seeds, "Time-domain computer modelling of opto-avalanche devices," presented at IEE Colloquium on CAD of Microwave Electron Devices with Time-Varying Fields, London, England, 1983, 1983/69, pp. 2.1–2.6.

[24] L. Picari and P. Spano, "New method for measuring ultrawide frequency response of optical detectors," *Electron. Lett.*, vol. 18, pp. 116–118, 1982.

Alwyn J. Seeds received the B.Sc. degree in electronics from Chelsea College, University of London, in 1976 and the Ph.D. degree in electrical engineering from University College London in 1980.

From 1980 to 1983 he was a Member of the Technical Staff at M.I.T. Lincoln Laboratory, where he worked on millimeter wave GaAs monolithic circuits. In 1983 he returned to England to take up a Lectureship at Queen Mary College, University of London, and in 1986 he was appointed to a Lectureship in the Department of Electronic and Electrical Engineering at University College London. His current research interests are in coherent optical systems, high speed optoelectronics and novel optoelectronic devices.

Dr. Seeds is a Chartered Engineer and a Member of the Institution of Electrical Engineering.

John F. Singleton received the B.Sc. degree in electronic and electrical engineering from the University of Surrey in 1970, the M.Sc. degree from the University of Salford in 1972, and the Ph.D. degree from Surrey in 1979.

He spent a number of years working on ion implantation of GaAs for FET and MMIC applications before transferring to oscillator development. He is now concerned with millimeter wave Gunn and IMPATT oscillator development at MEDL, Lincoln.

Sarah P. Brunt was born in Norfolk, England, on October 18, 1963. She received the B.Sc. degree (honours) in physics from the University of Leeds in June 1985.

Since then she has been working at Marconi Electronic Devices, Ltd., Lincoln, on IMPATT oscillator development.

John R. Forrest received the B.A. degree in electrical sciences from Cambridge University in 1964 and the D.Phil. degree from Oxford University in 1967, for work on the microwave properties of plasmas.

He was a Research Associate and Lecturer at Stanford University from 1967 to 1970, when he was appointed to a Lectureship in the Department of Electronic and Electrical Engineering at University College London. He was promoted to Reader in 1980 and to Professor in 1982. In 1984 he became Technical Director of Marconi Defence Systems, Ltd., and in 1986 he was appointed Director of Engineering for the Independent Broadcasting Authority. He has published extensively in the fields of phased array radar, printed antennas, satellite communications and the optical control of microwave systems.

Dr. Forrest is a Fellow and Member of the Council of the Institution of Electrical Engineers. He was appointed to the Fellowship of Engineering in 1985.

END

DATE
FILMED

11 87